lonephritis (case 3; 67 ys female) and liver abscess (case 4; 58 ys female). The patients were admitted to the university hospital or educational training hospitals in Okayama city from 2003 to 2004. The systolic and diastolic blood pressures before and after the treatment were 87.5 ± 20.2 and 48.3 ± 7.7 mmHg vs. 105.8 ± 29.2 and 56.3 ± 15.3 mmHg, respectively (mean $\pm$ SEM). The investigations were carried out with the approval of the ethical review committee of Okayama University Medical School. Written informed consent was obtained from the families of all patients.

The used PMX columns were washed with 500 ml of saline in the ICU. Then, the columns were cooled on ice and moved into a cold room at 4℃. The columns were successively washed with 500 ml of ice-cold saline at a flow rate of 16 ml/min 3 times, and the cells in each 500 ml fraction were analyzed. The columns were then opened and the cells attached to the filters were collected by shaking the filter in ice-cold saline. The collected cells from the fiber were smeared on the slide glass and subjected to May-Grunwald-Gimsa or immunocytochemical staining with PE-conjugated anti-CD14 and FITC-conjugated anti-CD68 antibodies. For scanning electron microscopic and transmission electron microscopic examinations, the PMX and the collected cells from the PMX column were fixed with 1% glutaraldehyde in 0.1 M phosphate buffer. FACS analysis was performed on the collected cells as well as peripheral blood mononuclear cells as described previously [5].

We found huge amounts of cellular components in the hemoperfused PMX columns from 4 patients (Fig. 1A). Fig. 1C shows the nuclear staining of leukocytes on the filter by hematoxylin when the filter was fixed immediately after opening the column. Fig. 1A is the corresponding picture made by scanning electron microscopy in which the cells include leukocytes and erythrocytes. About 70 to 80% of the total cells were recovered from the filter by gentle shaking in ice-cold saline (Figs. 1B and D). Fig. 2B clearly shows by May-Grunwald-Gimsa staining that the recovered leukocytes have the typical nuclear shape of monocytes with slight basophilic cytoplasm. Immunocytochemical staining confirmed that almost all leukocytes were immunoreactive for both CD14 and CD68 (Figs. 2C–F). The transmission electron microscopy also revealed that most of the cells recovered from the PMX filter have monocyte features polymorphic nuclei, few specific granules and many vacuoles (Fig. 3). Apoptotic changes such as nuclear condensation were not observed. These findings were common to four cases. Fig. 4 summarizes the leukocyte populations in the washings and in the PMX columns from four patients. Even in the washing fraction more than 75% cells were monocytes, although the cell numbers in the washings were less than 1% of those attached to the filter. The CD68 localization on the plasma membrane as well as within the cytoplasm (Fig. 2E) and the ultrastructural appearance of monocytes with irregularly shaped processes (Fig. 3) and numerous phagocytic vesicles strongly suggested that the monocytes trapped in the column had been activated through the pathological processes of septic shock. These results as a whole indicated that the PMX column specifically adsorbed monocytes (98.5% purity) among leukocytes from the peripheral blood of septic patients.

Analysis of the expression of adhesion molecules in monocytes from the peripheral blood as well as those recovered from PMX columns revealed that the expression levels of all adhesion molecules examined in patients were lower than those in normal volunteers (Fig. 5). The comparison of the expression levels of each adhesion molecule among monocytes from pre-treatment PBMC and those from PMX columns showed that the expression levels of CD11b in monocytes from PMX columns were lower than those in pre- and post-treatment PBMC. Also, CD62L expression in monocytes from PMX columns was lower than that in post-treatment PBMC. CD62L and CD11b, an α chain of the Mac-1 molecule, were considered to be involved in the cellular interaction therefore, the reduced levels of CD11b and 62L in monocytes in PMX columns may represent the shedding of these molecules after the stimulation of monocytes. Although the detailed phenotype features of bound monocytes are not known at present, it is quite likely that specific populations of monocytes show an increased affinity to PMX. It is not clear what enabled the monocytes with low levels of CD11b and CD62L to bind selectively to PMX. However, the removal of particular populations of monocytes from blood may provide a new strategy for the treatment of septic shock. Further research is necessary to confirm the causative relationship between the removal of specific

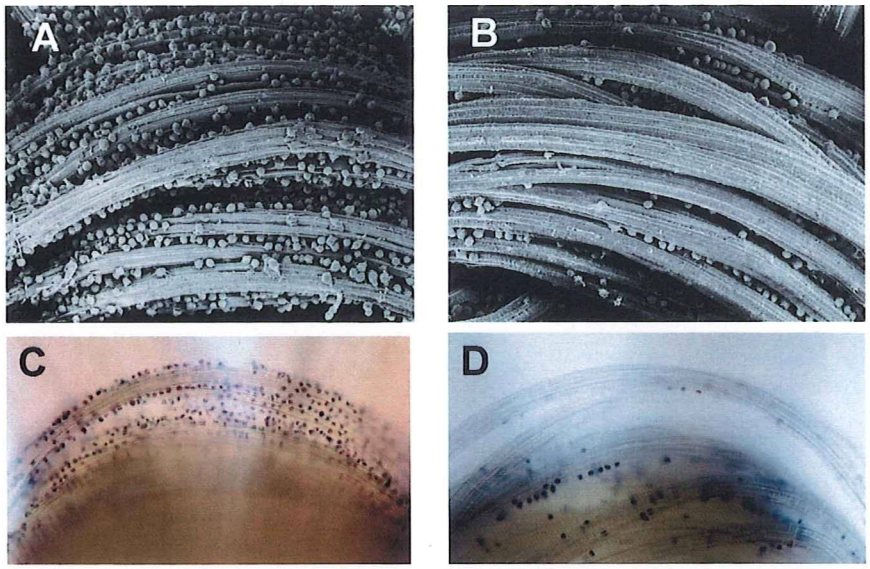

Fig. 1 Analysis of cellular components in the PMX columns. Scanning electron micrographs of the filter (A, B) and light micrographs of the hematoxylin-stained filter (C, D) show the cellular components in the PMX column before (A, C) and after the cells were collected (B, D). Numerous leukocytes were trapped on the filter, and a major portion of these cells were easily collected from the filter.

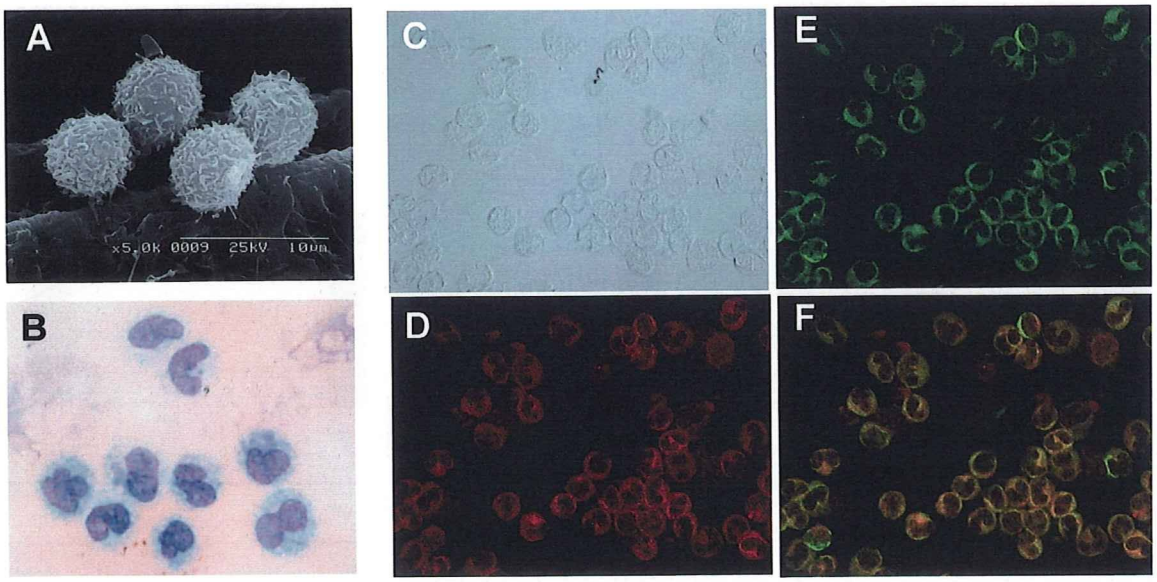

Fig. 2 Identification of leukocyte population. (A) Image of scanning electron microscopy of leukocytes on PMX filter. Smeared leukocytes from the column stained with May-Grunwald-Giemsa presented the typical monocyte appearance (B). Smeared samples (phase contrast image (C)) were immunostained with PE-conjugated anti-CDI4 (D) and FITC-conjugated anti-CD68 (E). Merged view (F). The specimen was from the patient identified as case 2.

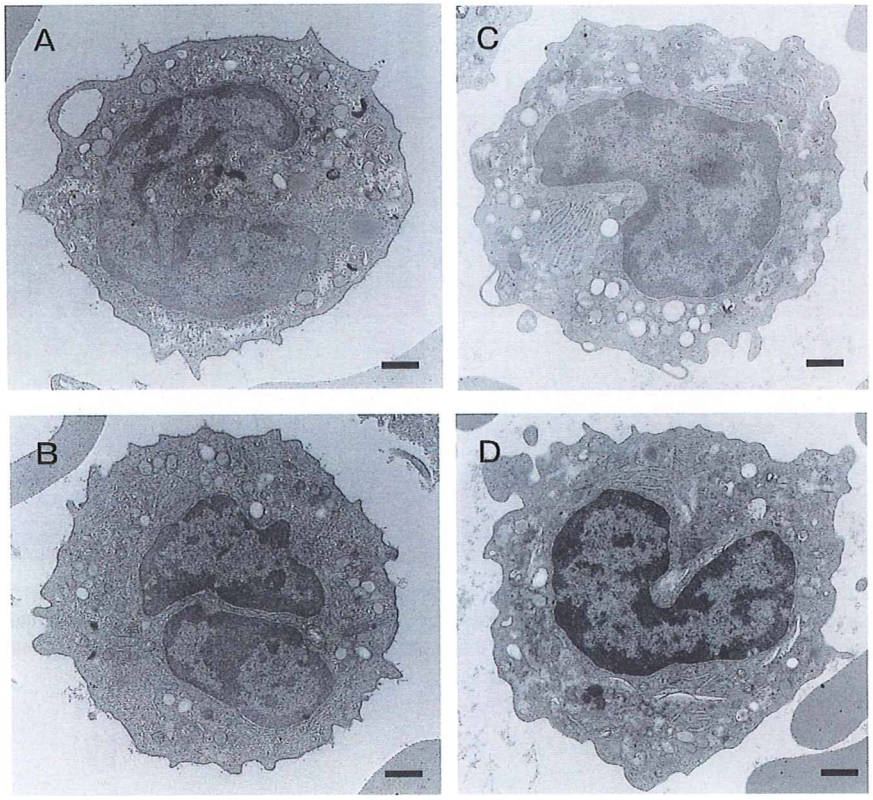

Fig. 3 Transmission electron micrograph of monocytes detached from the filter. The recovered leukocytes were fixed for transmission electron micrography. As shown in Fig. 2, most of the cells were monocytes. Four representative 4 cells are shown. There were vacuoles observed in the cytosol however, apoptotic changes such as condensation of nuclei were not present. The specimen was from the patient identified as case 2. Scale bars equal 1 μm.

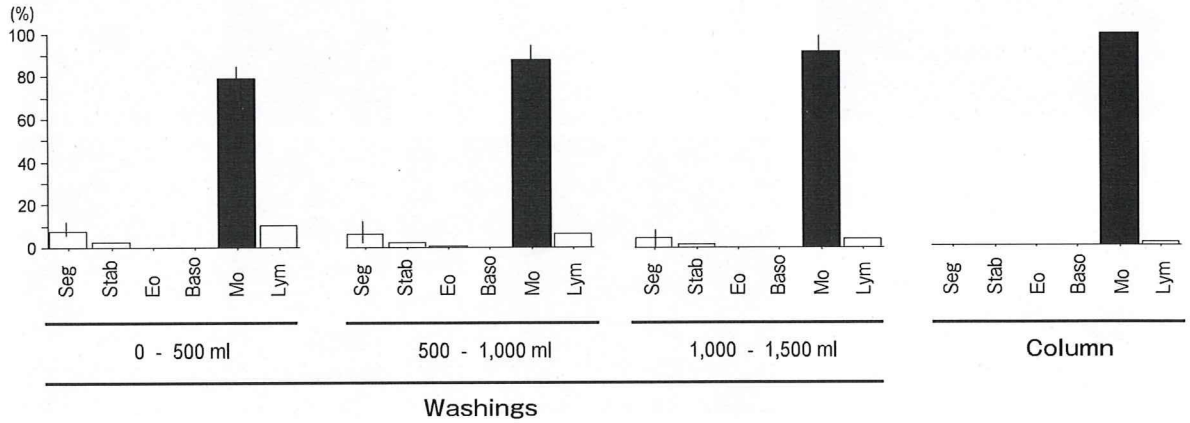

Fig. 4 Classification of leukocyte populations from washings and polymixin B-immobilized column. Smeared samples from each 500 ml washing and polymixin B-immobilized filter were used for the classification of leukocytes by May-Grunwald-Giemsa staining. The results are expressed as percentages of total cells (means ± SEM of 4 patients). Seg, segmented neutrophil; Stab, stab neutrophil; Eo, eosinophil; Baso, basophil; Mo, monocytes; Lym, lymphocyte.

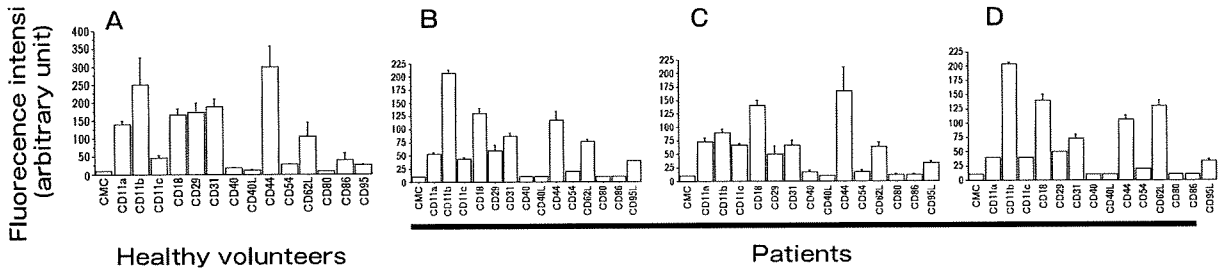

Fig. 5 FACS analysis of adhesion molecule expression on monocytes from healthy volunteers and patients. The peripheral blood was collected from 4 healthy volunteers (A) and patients before (B) and after (D) PMX treatment. PBMC was prepared from the peripheral blood. A diverse range of adhesion molecules on CD14-positive monocytes was analyzed by FACS. In C, the data on monocytes collected from PMX columns are shown. The data are the means ± SEM of 4 individuals.

monocytes and the beneficial effects of PMX treatment in septic shock.

References

1. Riedemann NC, Guo RF and Ward PA: Novel strategies for the treatment of sepsis. Nat Med (2003) 9: 517-524.
2. Bernard GR, Vincent JL, Laterre PF, LaRosa SP, Dhainaut JF, Lopez-Rodriguez A, Steingrub JS, Garber GE, Helterbrand JD, Ely EW and Fisher CJ Jr; Recombinant human protein C Worldwide Evaluation in Severe Sepsis (PROWESS) study group: Efficacy and safety of recombinant human activated protein C for severe sepsis. N Engl J Med (2001) 344: 699-709.
3. Shoji H: Extracorporeal endotoxin removal for the treatment of sepsis: endotoxin adsorption cartridge (Toraymyxin). Ther Apher Dial (2003) 7: 108-114.
4. Suzuki H, Nemoto H, Nakamoto H, Okada H, Sugahara S, Kanno Y and Moriwaki K: Continuous hemodiafiltration with polymyxin-B immobilized fiber is effective in patients with sepsis syndrome and acute renal failure. Ther Apher (2002) 6: 234-240.
5. Takahashi HK, Yoshida A, Iwagaki H, Yoshino T, Itoh H, Morichika T, Yokoyama M, Akagi T, Tanaka N, Mori S and Nishibori M: Histamine regulation of interleukin-18-initiating cytokine cascade is associated with down-regulation of intercellular adhesion molecule-1 expression in human peripheral blood mononuclear cells. J Pharmacol Exp Ther (2002) 300: 227-235.

0022-3565/09/3303-826–833$20.00
THE JOURNAL OF PHARMACOLOGY AND EXPERIMENTAL THERAPEUTICS

JPET 330:826–833, 2009

Vol. 330, No. 3
155960/3510190
Printed in U.S.A.

Histamine Inhibits Advanced Glycation End Products-Induced Adhesion Molecule Expression on Human Monocytes

Hidenori Wake, Hideo Kohka Takahashi, Shuji Mori, Keyue Liu, Tadashi Yoshino, and Masahiro Nishibori

Departments of Pharmacology (H.W., H.K.T., K.L., M.N.) and Pathology (T.Y.), Okayama University Graduate School of Medicine, Dentistry, and Pharmaceutical Sciences, Okayama, Japan; and Department of Pharmacy, Shujitsu University, Okayama, Japan (S.M.)

Received May 11, 2009; accepted June 26, 2009

ABSTRACT

Advanced glycation end products (AGEs) are modifications of proteins/lipids that become nonenzymatically glycated after contact with aldose sugars. Among various subtypes of AGEs, glyceraldehyde-derived AGE (AGE-2) and glycolaldehyde-derived AGE (AGE-3) are suggested to play roles in inflammation in diabetic patients. Because the engagement of intercellular adhesion molecule (ICAM)-1, B7.1, B7.2, and CD40 on monocytes with their ligands on T cells plays roles in cytokine production, we examined the effects of AGE-2 and AGE-3 on the expression of adhesion molecules and cytokine production in human peripheral blood mononuclear cells (PBMC) and their modulation by histamine in the present study. AGE-2 and AGE-3 induced the expressions of ICAM-1, B7.1, B7.2, and CD40 on monocytes and the production of interferon-γ in PBMC. Histamine concentration-dependently inhibited the action of AGE-2 and AGE-3. The effects of histamine were antagonized by an H2 receptor antagonist, famotidine, and mimicked by H2/H4 receptor agonists dimaprit and 4-methylhistamine. Histamine induced cAMP production in the presence and absence of AGE-2 and AGE-3. The effects of histamine were reversed by a protein kinase A (PKA) inhibitor, *N*-[2-(4-bromocinnamylamino)ethyl]-5-isoquinoline (H89), and mimicked by a dibutyryl cAMP and an adenylate cyclase activator, forskolin. These results as a whole indicated that histamine inhibited the AGE-2- and AGE-3-induced adhesion molecule expression and cytokine production via H2 receptors and the cAMP/PKA pathway.

AGEs are products of the nonenzymatic glycation/oxidation of proteins/lipids that accumulate during natural aging and are also greatly augmented in disorders such as diabetes, renal failure, and Alzheimer's disease (Schmidt et al., 1994; Brownlee, 1995; Takedo et al., 1996). AGEs are also implicated in the pathogenesis of atherosclerotic vascular disease of diabetic etiology (Takeuchi and Yamagishi, 2004). Direct immunochemical evidence for the existence of four distinct AGE structures, including AGE-2, AGE-3, AGE-4, and AGE-5, was identified, within the AGE-modified proteins and peptides (Takeuchi and Yamagishi, 2004). Among various subtypes of AGE, toxic AGE structures, AGE-2 and AGE-3, are the main structures of AGEs that are detectable in the serum of diabetic patients (Takeuchi and Yamagishi, 2004). AGE-2 is reported to induce diabetic microangiopathy (Takeuchi et al., 2000). AGE-2 and AGE-3 also have diverse biological activities on vascular wall cells, mesangial cells, Schwann cells, malignant melanoma cells, and cortical neurons (Okamoto et al., 2002; Yamagishi and Imaizumi, 2005). AGEs and the receptor for AGEs (RAGE) are detected in atherosclerotic plaque of diabetic patients (Cuccurullo et al., 2006). The stimulation of RAGE induces plaque rupture in diabetic patients. In vitro work has shown the involvement of RAGE, leading to oxidative stress and vascular damage, particularly in atherosclerosis (Vlassara and Palace, 2002) and in diabetes (Ruderman et al., 1992).

Microinflammation is a common major mechanism in the

This work was supported in part by grants from the Japan Society for the Promotion of Science [Grants 18590509, 20590539, 17659159, 19659061, 21659141, 21390071, 215905694]; the Scientific Research from Ministry of Health, Labour and Welfare of Japan; and the Takeda Science Foundation.

Article, publication date, and citation information can be found at http://jpet.aspetjournals.org.

doi:10.1124/jpet.109.155960.

ABBREVIATIONS: AGE, advanced glycation end product; RAGE, receptor for advanced glycation end product(s); IFN, interferon; PBMC, peripheral blood mononuclear cell(s); ICAM, intercellular adhesion molecule; H, histamine; PKA, protein kinase A; IL, interleukin; 4-MH, 4-methylhistamine dihydrochloride; BSA, bovine serum albumin; dbcAMP, dibutyryl cAMP; H89, *N*-[2-(4-bromocinnamylamino)ethyl]-5-isoquinoline; FITC, fluorescein isothiocyanate; mAb, monoclonal antibody; Ab, antibody; ELISA, enzyme-linked immunosorbent assay; sRAGE, soluble advanced glycosylation end product(s); LPS, lipopolysaccharide; NF-κB, nuclear factor-κB; SN50, H-Ala-Ala-Val-Ala-Leu-Leu-Pro-Ala-Val-Leu-Leu-Ala-Leu-Leu-Ala-Pro-Val-Gln-Arg-Lys-Arg-Gln-Lys-Leu-Met-Pro-OH; HDC, histidine decarboxylase.

pathogenesis of diabetic vascular complications. It is reported that diabetes has greater infiltration of macrophages and T cells in atherosclerotic plaques (Burke et al., 2004). Activation of monocytes/macrophages and T cells induces the progression of inflammatory atherosclerotic plaques (Stoll and Bendszus, 2006). It has been found that the enhancement of ICAM-1, B7.1, B7.2, and CD40 expression on monocytes results in the activation of T cells (Durie et al., 1994; Ranger et al., 1996; Camacho et al., 2001). Therefore, the blockade of engagement of adhesion molecules by antibodies against ICAM-1, B7.1, B7.2, and CD40 reduced the production of IFN-γ by PBMC (Morichika et al., 2003; Takahashi et al., 2003). In a previous study, we found that AGE-2 and AGE-3 induced the expression of ICAM-1, B7.1, B7.2, and CD40 on monocytes and production of IFN-γ in human PBMC, but AGE-4 and AGE-5 had no effect (Takahashi et al., 2009). The effect of AGE-2 and AGE-3 on the production of IFN-γ was dependent on cell-to-cell interaction via engagement between ICAM-1, B7.1, B7.2, and CD40 on monocytes and their ligands on T cells, and the stimulation of RAGE on monocytes was involved in the actions of AGE-2 and AGE-3 (Takahashi et al., 2009).

Histamine has immunoregulatory properties because it modulates cytotoxic T-cell activity (Khan et al., 1989), natural killer cell activity (Hellstrand et al., 1994), and cytokine production in PBMC (Dohlsten et al., 1987; Elenkov et al., 1998; van der Pouw Kraan et al., 1998). Histamine exerts its effects through the stimulation of H1, H2, H3, and H4 receptors (Elenkov et al., 1998; van der Pouw Kraan et al., 1998). In general, immunoregulatory effects of histamine depend on the stimulation of H2 receptors (Elenkov et al., 1998; van der Pouw Kraan et al., 1998; Hough, 2001). H2 receptor stimulation is coupled with the activation of adenylate cyclase and the cAMP/PKA pathway in monocytes (Shayo et al., 1997). However, little is known about the effect of histamine on the AGEs-induced activation of monocytes. In the present study, we examined the effect of histamine on the expressions of ICAM-1, B7.1, B7.2, and CD40 and the production of IFN-γ induced by AGE-2 and AGE-3.

Materials and Methods

Reagents and Drugs. Recombinant human IL-18 was purchased from Medical and Biological Laboratories (Nagoya, Japan). Histamine dihydrochloride was purchased from Nacalai Tesque (Kyoto, Japan). Dimaprit dihydrochloride and 4-methylhistamine dihydrochloride (4-MH) were gifts from Drs. W. A. M. Duncan and D. J. Durant (The Research Institute, Smith Kline and French Laboratories, Welwyn Garden City, Hertfordshire, UK). *d*-Chlorpheniramine maleate, ranitidine, and famotidine were provided by Yoshitomi Pharmaceutical Co. Ltd. (Tokyo, Japan), Glaxo Japan (Tokyo, Japan), and Yamanouchi Pharmaceutical Co. Ltd. (Tokyo, Japan), respectively. Thioperamide hydrochloride was provided by Eisai Co. Ltd. (Tokyo, Japan). AGE-modified bovine serum albumin (BSA) (Sigma-Aldrich, St. Louis, MO) was prepared as described previously (Takeuchi et al., 2000; Takahashi et al., 2009). In brief, each protein was incubated under sterile conditions with glyceraldehyde-3-phosphate (AGE-2) (Sigma-Aldrich) or glycolaldehyde (AGE-3) (Sigma-Aldrich) in 0.2 M phosphate buffer, pH 7.4, at 37°C for 7 days. AGE-BSA was dialyzed for 2 days at 4°C. The endotoxin concentration of AGEs at 100 μg/ml described above was measured at SRL (Okayama, Japan) and was found to be 1.2 pg/ml. AGE-specific fluorescence was measured at 450 nm after excitation at 390 nm with a fluorescence spectrophotometer (Hitachi, Tokyo, Japan). db-cAMP and forskolin were purchased from Wako Pure Chemicals (Tokyo, Japan). H89 was purchased from Sigma-Aldrich. For flow cytometric analysis, fluorescein isothiocyanate (FITC)-conjugated mouse IgG1 monoclonal antibody (mAb) against ICAM-1/CD54 and phycoerythrin-conjugated anti-CD14 mAb were purchased from Dako Denmark A/S (Glostrup, Denmark). FITC-conjugated mouse IgG1 mAb against B7.2 and CD40 were purchased from BD Biosciences Pharmingen (San Diego, CA), and FITC-conjugated IgG1, as an isotype-matched control, was obtained from Sigma-Aldrich.

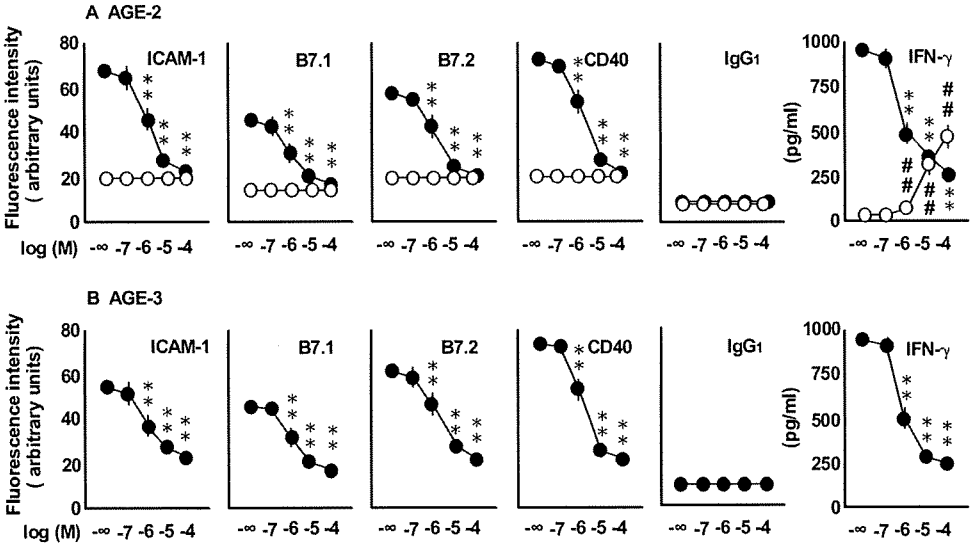

Fig. 1. Effects of histamine on the AGE-2- and AGE-3-induced expressions of ICAM-1, B7.1, B7.2, and CD40 on monocytes and production of IFN-γ in PBMC. PBMC at 1×10^6 cells/ml were incubated with AGE-2 (A) and AGE-3 (B) at 100 mg/ml and histamine at increasing concentrations from 0.1 to 100 μM for 24 h. The expressions of ICAM-1, B7.1, B7.2, and CD40 on monocytes were determined by flow cytometry. FITC-conjugated IgG1 was used as an isotype-matched control Ab. IFN-γ concentration in conditioned media was determined by ELISA. Filled circles (●) represent the effect of histamine on the adhesion molecule expression and cytokine production in the presence of AGE-2 and AGE-3. Open circles (○) represent the effect of histamine in the absence of AGE-2 and AGE-3. The results are expressed as the means ± S.E.M. of five donors with triplicate determinations. **, $P < 0.01$ compared with the value for AGE-2 and AGE-3. ##, $P < 0.01$ compared with the value for medium alone. When an error bar was within a symbol, the bar was omitted.

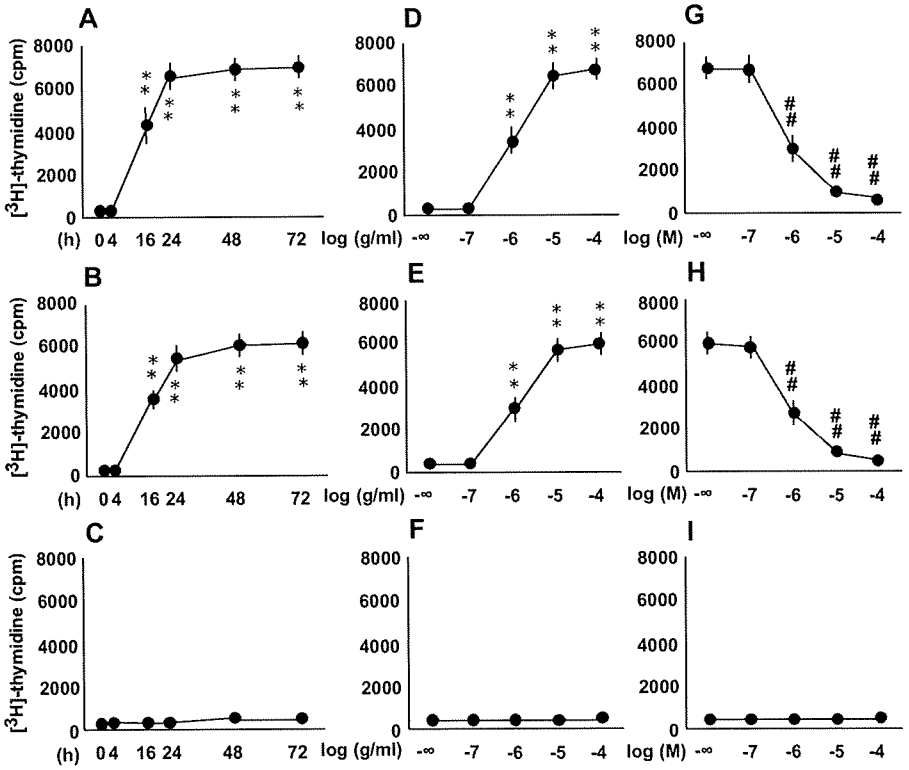

Fig. 2. Effects of histamine on the AGE-2- and AGE-3-induced lymphocyte proliferation. PBMC at 2×10^6 cells/ml were incubated with AGE-2 (A), AGE-3 (B), or BSA (C) at 100 μg/ml for the indicated periods, and the lymphocyte proliferation was determined by [^{3}H]thymidine uptake as described under *Materials and Methods*. The concentration-response relationships for the effects of AGE-2 (D), AGE-3 (E), or BSA (F) on the lymphocyte proliferation were determined at 24 h. The effects of increasing concentrations of histamine on 100 μg/ml AGE-2- (G), AGE-3- (H), or BSA (I)-induced lymphocyte proliferation were determined at 48 h. The results are expressed as the means ± S.E.M. of five donors with triplicate determinations. **, $P < 0.01$ compared with the value for 0 h (A–C) or 0 μg/ml (D–F). ##, $P < 0.01$ compared with the value in the presence of AGE-2 or AGE-3 alone.

Isolation of PBMC and Monocytes. Normal human PBMC were obtained from 10 healthy volunteers after acquiring institutional review board approval (Okayama University Institutional Review Board 106). Twenty to 50 ml of peripheral blood was withdrawn from a forearm vein, and PBMC were prepared from buffy coat as described previously (Takahashi et al., 2003). When monocytes were isolated from PBMC, counterflow centrifugal elutriation was used for separation as described previously (Takahashi et al., 2003). The PBMC and monocytes were then suspended at a final concentration of 1×10^6 cells/ml in the medium as described previously (Takahashi et al., 2003).

Flow Cytometric Analysis. Changes in the expression of human leukocyte antigens ICAM-1, B7.1, B7.2, and CD40 on monocytes were examined by multicolor flow cytometry using a combination of anti-CD14 Ab with anti-ICAM-1, anti-B7.1, anti-B7.2, or anti-CD40 Ab. PBMC at 1×10^6 cells/ml were incubated for 24 h. Cultured cells at 5×10^5 cells/ml were prepared for flow cytometric analysis as described previously (Takahashi et al., 2003) and analyzed with an FACSCalibur flow cytometer (BD Biosciences, San Jose, CA). The data were processed using the CellQuest program (BD Biosciences).

Cytokine Assay. PBMC at 1×10^6 cells/ml were used to analyze IFN-γ production. After culturing for 24 h at 37°C in a 5% CO_2/air mixture, cell-free supernatant was assayed for IFN-γ protein by enzyme-linked immunosorbent assay (ELISA) using the multiple Abs sandwich principle (R&D Systems, Minneapolis, MN). The detection limit of ELISA for IFN-γ was 10 pg/ml.

Proliferation Assay. PBMC were treated with various conditions. Cultures were incubated for 24 h, during which they were pulsed with [^{3}H]thymidine (3 Ci/well) for the final 16 h. Cells were then divided into 96-well microplates, 200 μl/well, resulting in 1 μCi of [^{3}H]thymidine per well and harvested by the Micro-Mate 196 cell harvester (PerkinElmer Life and Analytical Sciences, Boston, MA). Thymidine incorporation was measured by a beta-counter (Matrix 9600; PerkinElmer Life and Analytical Sciences).

Measurement of cAMP Production in Monocytes. Monocytes at 1×10^6 cells/ml were incubated at 37°C in a 5% CO_2/air mixture under different conditions. When the effects of histamine receptor antagonists were examined, the antagonists were added to the media 30 min before histamine addition. AGEs and histamine were simultaneously added to the media. After 24 h, cells at 2×10^5 cells/200 μl/well were supplemented with trichloroacetic acid to a final concentration of 5% and 3-isobutyl-1-methylxanthine, an inhibitor of phosphodiesterase, at 100 μM and frozen at −80°C. Frozen samples were subsequently sonicated and assayed for cAMP using a cAMP enzyme immunoassay kit (Cayman Chemical, Ann Arbor, MI) according to the manufacturer's instructions, for which no acetylation procedures were performed. The results are expressed as the means ± S.E.M. for five donors.

Statistical Examination. Statistical significance was evaluated using analysis of variance followed by Dunnett's test. A probability value of less than 0.05 was considered to indicate statistical significance. The results are expressed as the means ± S.E.M. of triplicate findings from five donors.

Results

Effects of Histamine on AGE-2- and AGE-3-Induced Expressions of ICAM-1, B7.1, B7.2, and CD40 on Monocytes; Production of IFN-γ; and Lymphocyte Proliferation in PBMC. In a previous study, to evaluate the binding of AGE subtypes to RAGE, we established an in vitro assay by using immobilized AGE subspecies and His-tagged sRAGE protein (Takahashi et al., 2009). AGE-2 and AGE-3 showed relatively high-affinity binding for sRAGE, whereas AGE-4 and AGE-5 showed moderate affinity for sRAGE. The proper incubation time and concentration of AGEs were determined according to Takahashi et al. (2009). AGE-2 and AGE-3 at 100 μg/ml significantly induced the expressions of ICAM-1, B7.1, B7.2, and CD40 and production of IFN-γ at 16 h and thereafter up to 24 and 48 h. As shown in Fig. 1, we observed the effects of histamine at concentrations ranging from 0.1 to 100 μM on the expression of ICAM-1, B7.1, B7.2,

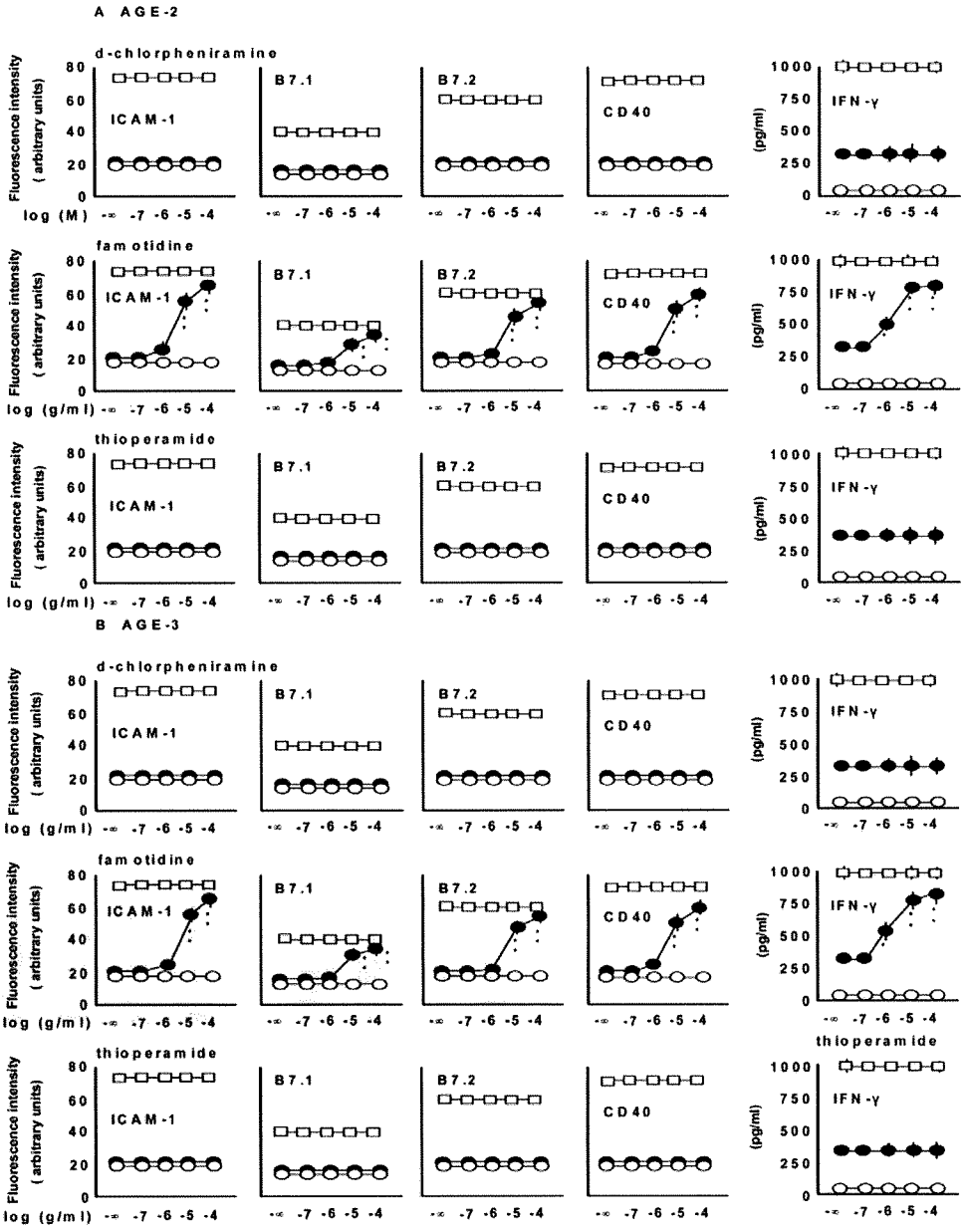

Fig. 3. Effects of histamine receptor antagonists on the histamine-induced inhibition of expressions of ICAM-1, B7.1, B7.2, and CD40 and production of IFN-γ. PBMC at 1×10^6 cells/ml were incubated with different classes of histamine receptor antagonists, including *d*-chlorpheniramine (H1 antagonist), famotidine (H2 antagonist), and thioperamide (H3/4 antagonist), at increasing concentrations from 0.1 to 100 μM in the presence or absence of AGE-2 (A) and AGE-3 (B) at 100 μg/ml. The expressions of ICAM-1, B7.1, B7.2, and CD40 on monocytes were determined by flow cytometry. In addition, IFN-γ concentration was determined by ELISA. Filled circles (●) represent the effect of antagonists on histamine-inhibited adhesion molecule expression and cytokine production in the presence of AGE-2 and AGE-3. Open squares (□) represent the effect of antagonists in the presence of AGE-2 and AGE-3 without histamine stimulation. Open circles (○) represent the effect of antagonists on adhesion molecule expression cytokine production in the absence of histamine, AGE-2, and AGE-3. The results are expressed as the means ± S.E.M. of five donors with triplicate determinations. *, $P < 0.05$; **, $P < 0.01$ compared with the value for histamine. When an error bar was within a symbol, the bar was omitted.

and CD40, the production of IFN-γ in the presence (100 μg/ml) or absence of AGE-2 and AGE-3 at 24 h. Moreover, AGE-2 and AGE-3 significantly induced the lymphocyte proliferation at 16 h and thereafter up to 24, 48, and 72 h (Fig. 2). The effect of histamine on lymphocyte proliferation was determined at 24 h.

Histamine concentration-dependently inhibited the AGE-2- and AGE-3-induced expressions of ICAM-1, B7.1, B7.2, and CD40; production of IFN-γ; and lymphocyte proliferation. The IC_{50} values for the inhibitory effect of histamine on the expressions of ICAM-1, B7.1, B7.2, and CD40, the production of IFN-γ, and the lymphocyte proliferation in the presence of AGE-2 were 1, 1, 1.5, 2, 0.8, and 0.8 μM, and those in the presence of AGE-3 were 1, 1, 1.7, 1.5, 0.8, and 0.8 μM, respectively. In the absence of AGE-2 and AGE-3, histamine induced the production of IFN-γ but had no effect on adhesion molecule expression and lymphocyte proliferation. The ED_{50} value for the effect of histamine alone on the production of IFN-γ was 4 μM.

Involvement of H2 Receptor in the Actions of Histamine. To determine the histamine receptor subtypes involved in the effects of histamine on the expressions of ICAM-1, B7.1, B7.2, and CD40 and the production of IFN-γ in the presence of AGE-2 and AGE-3, the effects of an H1 receptor antagonist *d*-chlorpheniramine; an H2 receptor antagonist, famotidine; and an H3/4 receptor antagonist, thioperamide, at concentrations ranging from 0.1 to 100 μM on adhesion molecule expression and cytokine production were examined in the presence of histamine at 100 μM (Fig. 3). Famotidine concentration-dependently inhibited the action of histamine, but *d*-chlorpheniramine and thioperamide had no effect. Another H2 receptor antagonist, ranitidine, exerted a substantially similar effect to famotidine (data not shown). As shown in Fig. 4, the effects of H2/H4 receptor agonists

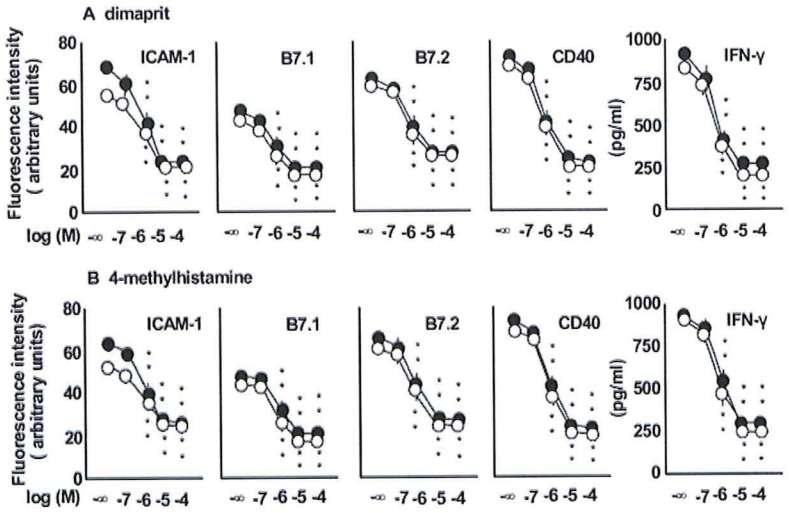

Fig. 4. Effects of histamine receptor agonists on the AGE-2- and AGE-3-induced expressions of ICAM-1, B7.1, B7.2, and CD40 and production of IFN-γ. PBMC at 1×10^6 cells/ml were incubated with histamine H2/H4 receptor agonists dimaprit (A) and 4-MH (B) at increasing concentrations from 0.1 to 100 μM in the presence of AGE-2 and AGE-3 at 100 μg/ml for 24 h. The expressions of ICAM-1, B7.1, B7.2, and CD40 on monocytes were determined by flow cytometry, and IFN-γ concentration in the conditioned media was determined by ELISA. Filled circles (●) represent the effect of agonists on AGE-2-induced responses, and open circles (○) represent AGE-3-induced responses. The results are expressed as the means ± S.E.M. of five donors with triplicate determinations. **, $P < 0.01$ compared with the value for AGE-2 or AGE-3 alone. When an error bar was within a symbol, the bar was omitted.

dimaprit and 4-MH (Parsons et al., 1977), at concentrations ranging from 0.1 to 100 μM, were determined in the presence of AGE-2 and AGE-3 at 100 μg/ml. Both dimaprit and 4-MH inhibited the expressions of ICAM-1, B7.1, B7.2, and CD40 and the production of IFN-γ in a concentration-dependent manner. The potency and efficacy of two agonists were quite similar to those of histamine in each response. Moreover, we found that an H1 agonist, 2-(2-pyridyl)ethylamine dihydrochloride (Durant et al., 1975), and an H3 agonist, (*R*)-α-methylhistamine dihydrochloride (Arrang et al., 1987), had no effect on the adhesion molecule expression and cytokine production induced by AGE-2 and AGE-3 (data not shown).

Effects of Histamine on the Production of cAMP in Monocytes in the Presence or Absence of AGE-2 and AGE-3. The effects of histamine at 100 μM on the production of intracellular cAMP in monocytes isolated from PBMC in the presence (100 μg/ml) or absence of AGE-2 and AGE-3 were determined (Fig. 5). Histamine induced the production of cAMP in monocytes with a peak 30 min after stimulation. The presence of AGE-2 and AGE-3 did not influence the production of cAMP induced by histamine. The H2 receptor antagonist famotidine at 100 μM inhibited the effect of histamine on the production of cAMP (Fig. 5). In addition, the H2/H4 receptor agonist dimaprit at 100 μM induced the production of cAMP (Fig. 5).

Involvement of cAMP in the Action of Histamine. To investigate the involvement of the cAMP/PKA pathway in the action of histamine, the effects of a PKA inhibitor, H89, at concentrations ranging from 0.1 to 100 μM, on the action of histamine at 100 μM were determined (Fig. 6). In the absence of histamine, the PKA inhibitor had no effect on adhesion molecule expression and cytokine expression. H89 reversed the inhibitory effect of histamine on the expressions of ICAM-1, B7.1, B7.2, and CD40 and the production of IFN-γ in the presence of AGE-2 or AGE-3. As shown in Fig. 7, the effects of a membrane-permeable cAMP analog, dbcAMP, and an adenylate cyclase activator, forskolin, at concentrations ranging from 0.1 to 100 μM, on the expressions of ICAM-1, B7.1, B7.2, and CD40 on monocytes and the production of IFN-γ in PBMC were examined. Both dbcAMP and forskolin inhibited the AGE-2- and AGE-3-induced adhesion molecule expression and cytokine production in a concentration-dependent manner.

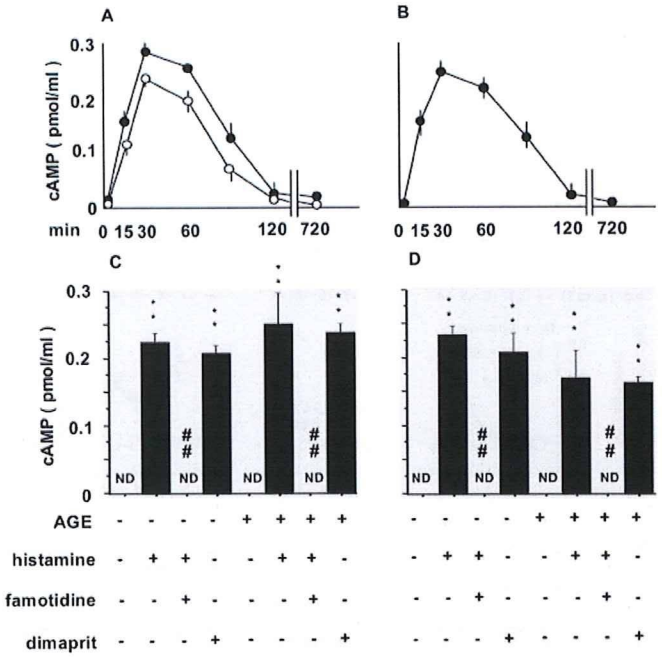

Fig. 5. Effects of histamine on the production of cAMP in monocytes in the presence or absence of AGE-2 and AGE-3. Monocytes at 1×10^6 cells/ml were incubated with histamine at 100 μM in the presence (filled circles; ●) and absence (open circles; ○) of AGE-2 (A) and AGE-3 (B) at 100 μg/ml, and time course changes in the levels of cAMP in monocytes were determined at the indicated time points. C, effects of histamine and dimaprit at 100 μM in combination with famotidine on the production of cAMP were determined in the presence or absence of AGE-2 at 100 μg/ml. D, effects of histamine and dimaprit at 100 μM in combination with famotidine on the production of cAMP were determined in the presence or absence of AGE-3 at 100 μg/ml. **, $P < 0.01$ compared with the corresponding value in the absence of histamine. ##, $P < 0.01$ compared with the corresponding value in the presence of histamine. The results are expressed as the means ± S.E.M. of five donors with triplicate determinations. When an error bar was within a symbol, the bar was omitted. ND, not detected.

Effect of Addition of IL-18 on Modulatory Effects of Histamine on AGE-2- and AGE-3-Induced ICAM-1 Expressions on Monocytes. The addition of increasing concentrations of IL-18 to the culture medium at the start of incubation antagonized the inhibitory effect of histamine at

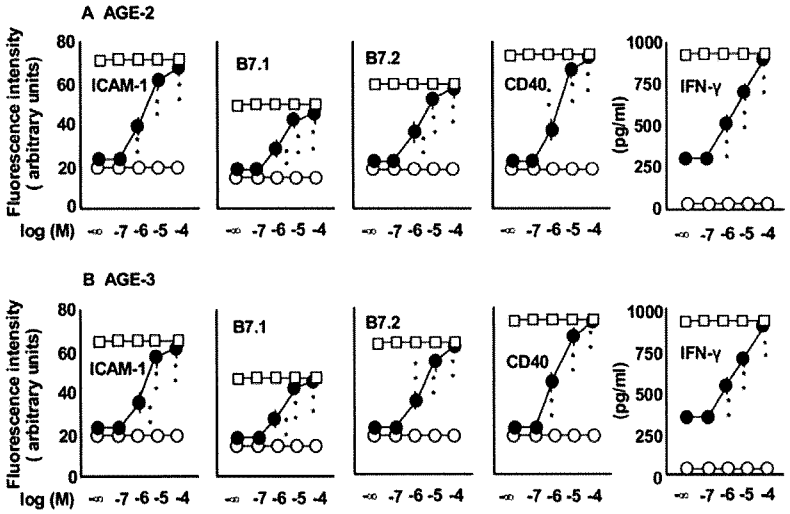

Fig. 6. Effects of PKA inhibitor on the histamine-induced expressions of ICAM-1, B7.1, B7.2, and CD40 and production of IFN-γ. The effects of a PKA inhibitor, H89, at increasing concentrations from 0.1 to 100 μM, on the 100 μM histamine-induced inhibition of expressions of ICAM-1, B7.1, B7.2, and CD40 and production of IFN-γ in the presence of AGE-2 (A) and AGE-3 (B) at 100 μg/ml were determined. Filled circles (●) represent the effect of H89 on the histamine-induced inhibition of responses in the presence of AGE-2 and AGE-3. Open squares (□) represent those in the presence of AGE-2 and AGE-3 without histamine stimulation. Open circles (○) represent the effect of H89 on the responses in the absence of both histamine and AGEs. The results are expressed as the means ± S.E.M. of triplicate findings from five donors. **, $P < 0.01$ compared with the value in the presence of histamine and AGEs. When an error bar was within a symbol, the bar was omitted.

100 μM on AGE-2- and AGE-3-induced ICAM-1 expression (Fig. 8).

Discussion

It is reported that the AGE-BSA enhances dendritic cell-induced stimulation of lymphocyte proliferation and cytokine production (Ge et al., 2005). In contrast, histamine inhibits lymphocyte proliferation and cytokine production via H2 receptors (Nakane et al., 2004). However, little is known about the effect of histamine on the actions of AGE-2 and AGE-3 in human PBMC. In the present study, we clearly demonstrated that histamine inhibited the AGE-2- and AGE-3-induced expressions of ICAM-1, B7.1, B7.2, and CD40 on human monocytes; production of IFN-γ; and lymphocyte proliferation in PBMC (Figs. 1 and 2). The action of histamine was inhibited by the H2 antagonist famotidine but not the H1 antagonist *d*-chlorpheniramine and the H3/4 antagonist thioperamide (Fig. 3). The H2/H4 receptor agonists dimaprit and 4-MH mimicked the action of histamine (Fig. 4). Because the IC_{50} values of histamine and H2/H4 receptor agonists to prevent the up-regulation of adhesion molecule expression and cytokine production were consistent with the affinity of those agonists to typical H2 receptors (Johnson, 1982; Elenkov et al., 1998; Kohka et al., 2000; Takahashi et al., 2002; Morichika et al., 2003), it was concluded that the inhibitory effect of histamine was mediated by the stimulation of H2 receptors but not H1, H3, and H4 receptors.

As shown in Fig. 5, histamine induced the production of cAMP in monocytes via H2 receptor irrespective of the presence of AGE-2 or AGE-3. The findings that the PKA inhibitor H89 inhibited the action of histamine (Fig. 6) and that the cAMP analog dbcAMP and the adenylate cyclase activator forskolin mimicked the effect of histamine (Fig. 7) strongly suggested the involvement of the cAMP/PKA pathway in the action of histamine.

We observed a similar pattern of inhibitory effects of histamine on lipopolysaccharide (LPS)- and IL-18-induced activation of monocytes in human PBMC via H2 receptors (Takahashi et al., 2002; Morichika et al., 2003). IL-18 is reported to induce the expressions of ICAM-1, B7.1, B7.2, and CD40 on monocytes (Takahashi et al., 2002, 2003). Although AGE-2 and AGE-3 do not induce production of IL-18 in PBMC (Takahashi et al., 2009), histamine induces production of IL-18 via H2 receptor and the cAMP/PKA pathway in monocytes (Takahashi et al., 2006). Thus, there may be a common pathway triggered by LPS, IL-18, and AGEs that

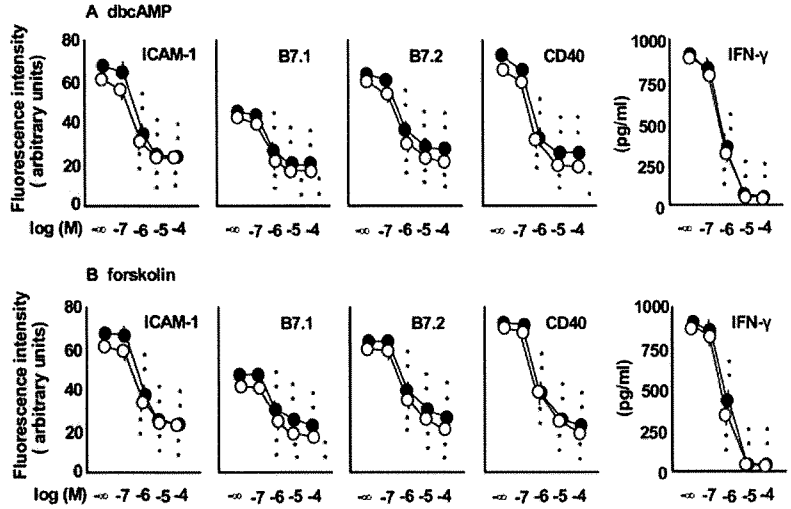

Fig. 7. Effects of forskolin and dbcAMP on AGEs-induced expressions of ICAM-1, B7.1, B7.2, and CD40 on monocytes and production of IFN-γ in PBMC. PBMC at 1×10^6/ml were incubated with a cAMP analog, dbcAMP (A), and an adenylate cyclase activator, forskolin (B), at increasing concentrations from 0.1 to 100 μM in the presence of AGE-2 and AGE-3 at 100 μg/ml for 24 h. Filled circles (●) represent the effects of dbcAMP or forskolin on AGE-2-induced responses, and open circles (○) represent the effects of dbcAMP or forskolin on the AGE-3-induced responses. The results are expressed as the means ± S.E.M. of five donors with triplicate determinations. **, $P < 0.01$ compared with the value for AGE-2 or AGE-3 alone. When an error bar was within a symbol, the bar was omitted.

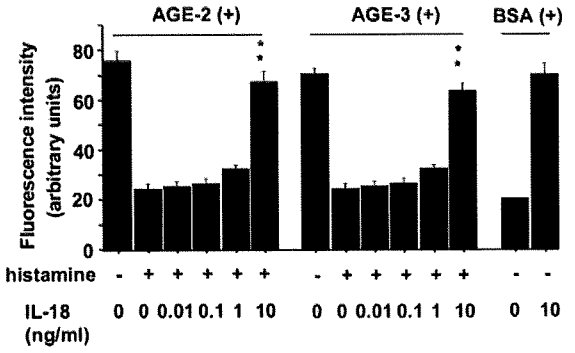

Fig. 8. Effect of IL-18 on the modulatory effects of histamine on AGE-2- and AGE-3-induced ICAM-1 expression on monocytes. PBMC at 1×10^6 cells/ml were incubated with IL-18 at increasing concentrations from 0.01 to 10 ng/ml in the absence or presence of AGE-2 and AGE-3 at 100 μg/ml and histamine at 100 μM for 24 h. At the end of the culture, the expressions of ICAM-1 were determined by flow cytometry. The results are expressed as the means ± S.E.M. of five donors with triplicate determinations. **, $P < 0.01$ compared with the value for histamine.

was regulated by the H2 receptors-cAMP/PKA system. Further work is necessary on this issue.

Although AGE-2 and AGE-3 do not induce production of IL-18 in PBMC (Takahashi et al., 2009), histamine induces production of IL-18 via H2 receptor and the cAMP/PKA pathway in monocytes (Takahashi et al., 2006). The amount of IL-18 production induced by histamine at 100 μM was 2.5 ng/ml. IL-18 is reported to induce the expressions of ICAM-1, B7.1, B7.2, and CD40 on monocytes (Takahashi et al., 2002, 2003). As shown in Fig. 8, the requirement of relatively higher concentration of exogenous IL-18 for reversing the inhibitory effect of histamine on AGE-2- and AGE-3-induced action may reflect the IL-18 concentration needed for the functional antagonism of histamine action on ICAM-1 expression. The regulatory mechanisms for ICAM-1 expression in the presence of plural stimuli should be clarified.

In the previous study, we found that AGE-2 and AGE-3 have higher affinity for RAGE than AGE-4 and AGE-5 by using an in vitro binding assay (Takahashi et al., 2009). AGE-2 and AGE-3, but not AGE-4 and AGE-5, induced the up-regulation of their receptor RAGE expression on the cell surface of monocytes. A NF-κB activation inhibitor, SN50, inhibits AGE-2- and AGE-3-induced adhesion molecule expressions and cytokine production (Takahashi et al., 2009), and the interaction of AGE and RAGE enhances the expression of RAGE through activation of NF-κB in monocytes (Li and Schmidt, 1997). However, histamine had no effect on the expression of RAGE in the presence and absence of AGE-2 and AGE-3 (data not shown). Thus, it might be possible that the downstream pathways of NF-κB activation leading to up-regulation of adhesion molecules and RAGE are probably differentially regulated by the cAMP-PKA system.

Histidine decarboxylase (HDC), which produces histamine from L-histidine, is detected in monocytes/macrophages located in the arterial intima in human atherosclerotic lesions (Higuchi et al., 2001). In a rat model of streptozotocin-induced diabetes mellitus, histamine levels are elevated in various tissues, including the aorta (Gill et al., 1990). Moreover, vascular smooth muscle cells express HDC after injury to endothelial cells (Sasaguri et al., 2005). The resultant production of histamine may regulate vascular contraction directly or indirectly via nitric oxide production (Tanimoto et al., 2007). In addition to the control of vascular contraction, the modulatory effects of histamine on microinflammation in atherosclerotic intima through the regulation of monocytes/macrophages are shown in the present study. In fact, AGEs have been demonstrated in atherosclerotic plaque, where macrophages with up-regulated RAGE are present (Cuccurullo et al., 2006). Therefore, the regulatory action of histamine through the stimulation of H2 receptors may inhibit the macrophage-mediated events stimulated by AGE-2 and AGE-3, including the production of IFN-γ and adhesion molecule-dependent activation of T cells (Takahashi et al., 2009). Thus, locally produced histamine may exert inhibitory influence on the secretory response of macrophages and T-cell activation, leading to the reduction of atherosclerotic plaque formation. Such a possibility should be evaluated by an in vivo atherosclerotic model. It is reported that atherosclerotic lesions are reduced in HDC-knockout mice, compared with wild-type mice (Tanimoto et al., 2006). However, in HDC-knockout mice, the deficiency of granule formation and proteinases expression in mast cells is also observed (Ohtsu et al., 2002). Therefore, attention should be paid to obtaining a straightforward explanation for the phenotype of knockout mice.

It is reported that an H1 receptor antagonist, diphenhydramine, reduces the formation of intimal hyperplasia in a mouse model with endothelial injury; however, an H2 receptor antagonist, cimetidine, is ineffective (Miyazawa et al., 1998). Cimetidine inhibits neither the proliferation nor migration of mouse vascular smooth muscle cells stimulated by platelet-derived growth factor, whereas diphenhydramine significantly inhibited proliferation but did not inhibit migration (Miyazawa et al., 1998). Therefore, stimulation of H1 receptor may induce the proliferation of vascular smooth muscle cells, whereas H2 receptor stimulation may inhibit the activation of monocytes, leading to the prevention of atherosclerosis. Further study of the role of H1 and H2 receptor stimulation should be continued.

In conclusion, histamine inhibited the AGE-2- and AGE-3-induced expressions of ICAM-1, B7.1, B7.2, and CD40 and production of IFN-γ via H2 receptors and the cAMP/PKA pathway. Through the inhibition of toxic AGE-dependent responses in monocytes, the stimulation of H2 receptors may partially contribute to regulating the development of atherosclerotic plaques in diabetes.

Acknowledgments

We thank Miyuki Shiotani and Yukinari Isomoto for technical assistance.

References

Arrang JM, Garbarg M, Lancelot JC, Lecomte JM, Pollard H, Robba M, Schunack W, and Schwartz JC (1987) Highly potent and selective ligands for histamine H3-receptors. *Nature* **327**:117–123.

Brownlee M (1995) Advanced protein glycosylation in diabetes and aging. *Annu Rev Med* **46**:223–234.

Burke AP, Kolodgie FD, Zieske A, Fowler DR, Weber DK, Varghese PJ, Farb A, and Virmani R (2004) Morphologic findings of coronary atherosclerotic plaques in diabetics: a postmortem study. *Arterioscler Thromb Vasc Biol* **24**:1266–1271.

Camacho SA, Heath WR, Carbone FR, Sarvetnick N, LeBon A, Karlsson L, Peterson PA, and Webb SR (2001) A key role for ICAM-1 in generating effector cells mediating inflammatory responses. *Nat Immunol* **2**:523–529.

Cuccurullo C, Iezzi A, Fazia ML, De Cesare D, Di Francesco A, Muraro R, Bei R, Ucchino S, Spigonardo F, Chiarelli F, et al. (2006) Suppression of RAGE as a basis of simvastatin-dependent plaque stabilization in type 2 diabetes. *Arterioscler Thromb Vasc Biol* **26**:2716–2723.

Dohlsten M, Sjogren HO, and Carlsson R (1987) Histamine acts directly on human T cells to inhibit interleukin-2 and interferon-gamma production. *Cell Immunol* **109**:65–70.

Durant GJ, Ganellin CR, and Parsons ME (1975) Chemical differentiation of histamine H1- and H2-receptor agonists. *J Med Chem* **18:**905–909.
Durie FH, Foy TM, Masters SR, Laman JD, and Noelle RJ (1994) The role of CD40 in the regulation of humoral and cell-mediated immunity. *Immunol Today* **15:** 406–411.
Elenkov IJ, Webster E, Papanicolaou DA, Fleisher TA, Chrousos GP, and Wilder RL (1998) Histamine potently suppresses human IL-12 and stimulates IL-10 production via H2 receptors. *J Immunol* **161:**2586–2593.
Ge J, Jia Q, Liang C, Luo Y, Huang D, Sun A, Wang K, Zou Y, and Chen H (2005) Advanced glycosylation end products might promote atherosclerosis through inducing the immune maturation of dendritic cells. *Arterioscler Thromb Vasc Biol* **25:**2157–2163.
Gill DS, Thompson CS, and Dandona P (1990) Histamine synthesis and catabolism in various tissues in diabetic rats. *Metabolism* **39:**815–818.
Hellstrand K, Asea A, Dahlgren C, and Hermodsson S (1994) Histaminergic regulation of NK cells. Role of monocyte-derived reactive oxygen metabolites. *J Immunol* **153:**4940–4947.
Higuchi S, Tanimoto A, Arima N, Xu H, Murata Y, Hamada T, Makishima K, and Sasaguri Y (2001) Effects of histamine and interleukin-4 synthesized in arterial intima on phagocytosis by monocytes/macrophages in relation to atherosclerosis. *FEBS Lett* **505:**217–22.
Hough LB (2001) Genomics meets histamine receptors: new subtypes, new receptors. *Mol Pharmacol* **59:**415–419.
Johnson CL (1982) Histamine receptors and cyclic nucleotides, in *Pharmacology of Histamine Receptors* (Ganellin CR and Parsons ME, eds) p 146, Wright-PSG, Bristol, UK.
Khan MM, Keaney KM, Melmon KL, Clayberger C, and Krensky AM (1989) Histamine regulates the generation of human cytolytic T lymphocytes. *Cell Immunol* **121:**60–73.
Kohka H, Nishibori M, Iwagaki H, Nakaya N, Yoshino T, Kobashi K, Saeki K, Tanaka N, and Akagi T (2000) Histamine is a potent inducer of IL-18 and IFN-gamma in human peripheral blood mononuclear cells. *J Immunol* **164:**6640–6646.
Li J and Schmidt AM (1997) Characterization and functional analysis of the promoter of RAGE, the receptor for advanced glycation end products. *J Biol Chem* **272:**16498–16506.
Miyazawa N, Watanabe S, Matsuda A, Kondo K, Hashimoto H, Umemura K, and Nakashima M (1998) Role of histamine H1 and H2 receptor antagonists in the prevention of intimal thickening. *Eur J Pharmacol* **362:**53–59.
Morichika T, Takahashi HK, Iwagaki H, Yoshino T, Tamura R, Yokoyama M, Mori S, Akagi T, Nishibori M, and Tanaka N (2003) Histamine inhibits lipopolysaccharide-induced tumor necrosis factor-alpha production in an intercellular adhesion molecule-1- and B7.1-dependent manner. *J Pharmacol Exp Ther* **304:**624–633.
Nakane H, Sonobe Y, Watanabe T, and Nakano K (2004) Histamine: its novel role as an endogenous regulator of Con A-dependent T cell proliferation. *Inflamm Res* **53:**324–328.
Ohtsu H, Kuramasu A, Tanaka S, Terui T, Hirasawa N, Hara M, Makabe-Kobayashi Y, Yamada N, Yanai K, Sakurai E, et al. (2002) Plasma extravasation induced by dietary supplemented histamine in histamine-free mice. *Eur J Immunol* **32:**1698–1708.
Okamoto T, Yamagishi S, Inagaki Y, Amano S, Koga K, Abe R, Takeuchi M, Ohno S, Yoshimura A, and Makita Z (2002) Angiogenesis induced by advanced glycation end products and its prevention by cerivastatin. *FASEB J* **16:**1928–1930.
Parsons ME, Owen DA, Ganellin CR, and Durant GJ (1977) Dimaprit—(*S*-[3-(*N*,*N*-dimethylamino)prophyl]isothiourea)—a highly specific histamine H2-receptor agonist. Part 1. Pharmacology. *Agents Actions* **7:**31–37.
Ranger AM, Das MP, Kuchroo VK, and Glimcher LH (1996) B7-2 (CD86) is essential for the development of IL-4-producing T cells. *Int Immunol* **8:**1549–1560.
Ruderman NB, Williamson JR, and Brownlee M (1992) Glucose and diabetic vascular disease. *FASEB J* **6:**2905–2914.
Sasaguri Y, Wang KY, Tanimoto A, Tsutsui M, Ueno H, Murata Y, Kohno Y, Yamada S, and Ohtsu H (2005) Role of histamine produced by bone marrow-derived vascular cells in pathogenesis of atherosclerosis. *Circ Res* **96:**974–981.
Schmidt AM, Hasu M, Popov D, Zhang JH, Chen J, Yan SD, Brett J, Cao R, Kuwabara K, Costache G, Simonescut N, Simonescut M, and Stern D (1994) Receptor for advanced glycation end products (AGEs) has a central role in vessel wall interactions and gene activation in response to circulating AGE proteins. *Proc Natl Acad Sci USA* **91:**8807–8811.
Shayo C, Davio C, Brodsky A, Mladovan AG, Legnazzi BL, Rivera E, and Baldi A (1997) Histamine modulates the expression of c-fos through cyclic AMP production via the H2 receptor in the human promonocytic cell line U937. *Mol Pharmacol* **51:**983–990.
Stoll G and Bendszus M (2006) Inflammation and atherosclerosis: novel insights into plaque formation and destabilization. *Stroke* **37:**1923–1932.
Takahashi HK, Iwagaki H, Tamura R, Xue D, Sano M, Mori S, Yoshino T, Tanaka N, and Nishibori M (2003) Unique regulation profile of prostaglandin E1 on adhesion molecule expression and cytokine production in human peripheral blood mononuclear cells. *J Pharmacol Exp Ther* **307:**1188–1195.
Takahashi HK, Mori S, Wake H, Liu K, Yoshino T, Ohashi K, Tanaka N, Shikata K, Makino H, and Nishibori M (2009) Advanced glycation end products subspecies-selectively induce adhesion molecule expression and cytokine production in human peripheral blood mononuclear cells. *J Pharmacol Exp Ther* **330:**89–98.
Takahashi HK, Watanabe T, Yokoyama A, Iwagaki H, Yoshino T, Tanaka N, and Nishibori M (2006) Cimetidine induces interleukin-18 production through H2-agonist activity in monocytes. *Mol Pharmacol* **70:**450–453.
Takahashi HK, Yoshida A, Iwagaki H, Yoshino T, Itoh H, Morichika T, Yokoyama M, Akagi T, Tanaka N, Mori S, et al. (2002) Histamine regulation of interleukin-18-initiating cytokine cascade is associated with down-regulation of intercellular adhesion molecule-1 expression in human peripheral blood mononuclear cells. *J Pharmacol Exp Ther* **300:**227–235.
Takedo A, Yasuda T, Miyata T, Mizuno K, Li M, Yoneyama S, Horie K, Maeda K, and Sobue G (1996) Immunohistochemical study of advanced glycation end products in aging and Alzheimer's disease brain. *Neurosci Lett* **221:**17–20.
Takeuchi M and Yamagishi S (2004) TAGE (toxic AGEs) hypothesis in various chronic diseases. *Med Hypotheses* **63:**449–452.
Takeuchi M, Makita Z, Bucala R, Suzuki T, Koike T, and Kameda Y (2000) Immunological evidence that non-carboxymethyllysine advanced glycation end-products are produced from short chain sugars and dicarbonyl compounds in vivo. *Mol Med* **6:**114–125.
Tanimoto A, Sasaguri Y, and Ohtsu H (2006) Histamine network in atherosclerosis. *Trends Cardiovasc Med* **16:**280–284.
Tanimoto A, Wang KY, Murata Y, Kimura S, Nomaguchi M, Nakata S, Tsutsui M, and Sasaguri Y (2007) Histamine upregulates the expression of inducible nitric oxide synthase in human intimal smooth muscle cells via histamine H1 receptor and NF-kappaB signaling pathway. *Arterioscler Thromb Vasc Biol* **27:**1556–1561.
van der Pouw Kraan TC, Snijders A, Boeije LC, de Groot ER, Alewijnse AE, Leurs R, and Aarden LA (1998) Histamine inhibits the production of interleukin-12 through interaction with H2 receptors. *J Clin Invest* **102:**1866–1873.
Vlassara H and Palace MR (2002) Diabetes and advanced glycation endproducts. *J Intern Med* **251:**87–101.
Yamagishi S and Imaizumi T (2005) Diabetic vascular complications: pathophysiology, biochemical basis and potential therapeutic strategy. *Curr Pharm Des* **11:** 2279–2299.

Address correspondence to: Dr. Masahiro Nishibori, Department of Pharmacology, Okayama University Graduate School of Medicine and Dentistry, 2-5-1 Shikata-cho, Okayama 700-8558, Japan. E-mail: mbori@md.okayama-u.ac.jp

Acta Med. Okayama, 2009
Vol. 63, No. 4, pp. 203-211

Acta Medica Okayama
http://escholarship.lib.okayama-u.ac.jp/amo/

Original Article

Establishment of *in Vitro* Binding Assay of High Mobility Group Box-1 and S100A12 to Receptor for Advanced Glycation Endproducts: Heparin's Effect on Binding

Rui Liu[a,b], Shuji Mori[c], Hidenori Wake[b], Jiyong Zhang[b], Keyue Liu[b], Yasuhisa Izushi[b], Hideo K. Takahashi[b], Bo Peng[a], and Masahiro Nishibori[b]*

[a]*Shanghai University of Traditional Chinese Medicine, Shanghai 201-203, China,* [b]*Department of Pharmacology, Okayama University Graduate School of Medicine, Dentistry and Pharmaceutical Sciences, Okayama 700-8558, Japan, and* [c]*Shujitsu University, School of Pharmacy, Okayama 703-8516, Japan*

Interaction between the receptor for advanced glycation end products (RAGE) and its ligands has been implicated in the pathogenesis of various inflammatory disorders. In this study, we establish an *in vitro* binding assay in which recombinant human high-mobility group box 1 (rhHMGB1) or recombinant human S100A12 (rhS100A12) immobilized on the microplate binds to recombinant soluble RAGE (rsRAGE). The rsRAGE binding to both rhHMGB1 and rhS100A12 was saturable and dependent on the immobilized ligands. The binding of rsRAGE to rhS100A12 depended on Ca^{2+} and Zn^{2+}, whereas that to rhHMGB1 was not. Scatchard plot analysis showed that rsRAGE had higher affinity for rhHMGB1 than for rhS100A12. rsRAGE was demonstrated to bind to heparin, and rhS100A12, in the presence of Ca^{2+}, was also found to bind to heparin. We examined the effects of heparin preparations with different molecular sizes—unfractionated native heparin (UFH), low molecular weight heparin (LMWH) 5000 Da, and LMWH 3000 Da— on the binding of rsRAGE to rhHMGB1 and rhS100A12. All 3 preparations concentration-dependently inhibited the binding of rsRAGE to rhHMGB1 to a greater extent than did rhS100A12. These results suggested that heparin's anti-inflammatory effects can be partly explained by its blocking of the interaction between HMGB1 or S100A12 and RAGE. On the other hand, heparin would be a promising effective remedy against RAGE-related inflammatory disorders.

Key words: RAGE, HMGB1, S100A12, heparin, inflammation

The receptor for advanced glycation end products (RAGE) is a member of the immunoglobulin superfamily of cell-surface molecules, which has been suggested to be involved in sustaining and amplifying inflammatory responses [1, 2]. RAGE can recognize a wide range of endogenous ligands, such as advanced glycation end products (AGEs), amyloid-β peptide (A β), high mobility group box 1 (HMGB1), and the S100/calgranulin family [3]. RAGE's structure includes an extracellular immunoglobulin-like region essential for its binding to ligands, a single transmembrane domain, and a short cytoplasmic tail responsible for RAGE-mediated signal transduction [4]. There are soluble forms of RAGE—endogenous secretory RAGE (esRAGE) and soluble RAGE (sRAGE)—that lack a transmembrane domain and act

Received April 22, 2009; accepted June 23, 2009.
*Corresponding author. Phone:+81-86-235-7140; Fax:+81-86-235-7140
E-mail:mbori@md.okayama-u.ac.jp (M. Nishibori)

as decoy receptors [5]. The binding of ligands to RAGE triggers intracellular signaling such as nuclear factor kappa B (NF-κB) and mitogen-activated protein kinase (MAPK) activation in vascular endothelial cells and macrophages, leading to the development of inflammation-based diseases, such as diabetic complications, sepsis, Alzheimer's and rheumatic arthritis [6-9]. As a result, interfering with the binding of ligands to RAGE has been thought to be a means with which to block the inflammatory responses sustained by RAGE-dependent pathways.

Among the RAGE ligands, AGEs are the groups of nonenzymatically glycosylated proteins that accumulate in vascular tissue in a wide variety of disorders, especially in diabetes [10]. HMGB1 is a ubiquitous and abundant nuclear protein, which can be passively released from necrotic cells and actively secreted by macrophages. After HMGB1 is released into the extracellular environment, it functions as a pro-inflammatory mediator [11, 12]. S100/calgranulin is a multigenic family of EF-hand Ca^{2+}-binding proteins [13]. S100A12 is one member of the S100 protein family, which is found mainly in neutrophil granulocytes and monocytes [14]. S100A12 has a role in cell homeostasis as an intracellular molecule, but contributes to the pathogenesis of inflammatory lesions via interaction with RAGE after release to the extracellular compartment [15].

Heparin is a highly sulfated glycosaminoglycan, which has been traditionally used clinically as an anticoagulant [16]. It is biosynthesized and stored in the granules of mast cells [17]. More recent studies have highlighted the role of heparin as an anti-inflammatory substance that has been used in the treatment of some inflammatory settings [18-20]. However, the molecular mechanisms underlying the anti-inflammation activities of heparin remain to be determined. Antagonism of AGE's effect by LMWH *in vivo* has been reported [21]. A similar effect of heparin on AGE-RAGE signaling also has been demonstrated by the inhibition of RAGE-dependent NF-κB activation in glioma cells and expression of vascular cell adhesion molecule-1 (VCAM-1) and vascular endothelial growth factor (VEGF) in endothelial cells. HMGB1 has also been described as a heparin-binding protein [22-24]. Therefore, heparin may be an important regulator of RAGE-mediated responses through multiple ligands.

To investigate the complex binding properties of RAGE to many ligands, we attempted to establish *in vitro* binding of sRAGE to HMGB1 and S100A12 using a microplate. Both *in vitro* binding assays were saturated in terms of sRAGE and ligands. We clearly showed Ca^{2+}, Zn^{2+}-dependent binding of S100A12 to sRAGE. We also observed the binding inhibition activity of each of the 3 heparin preparations, suggesting a mechanism for heparin's anti-inflammatory activity. This may provide insights into potential uses of heparin in some RAGE-related pathologies.

Materials and Methods

Materials. Recombinant plasmid pASK-IBA32-sRAGE was transformed into *E.coli* BL 21 (DE3) (Merck, San Diego, LA), and recombinant sRAGE (rsRAGE) proteins with a 6-histidine tag were expressed. rsRAGE proteins were partially purified by using a Ni-NTA column and further purified by heparin-sepharose affinity chromatography. Recombinant plasmids pGEX-6P-1-HMGB1 and pGEX-6P-1-S100A12 were transformed into *E.coli* BL 21 (DE3). Recombinant human HMGB1 (rhHMGB1) and recombinant human S100A12 (rhS100A12) proteins were expressed as GST-HMGB1 or GST-S100A12 fusion proteins, respectively. GST tag was cleaved by protease in Glutathione Sepharose™ 4B columns. Unfractionated heparin (UFH) (mol wt: 12000~15000 Da), low molecular weight heparin (LMWH) (mol wt: 5000 Da or 3000 Da), and bovine serum albumin (BSA) were purchased from Sigma-Aldrich (St. Louis, MO, USA). 2, 2'-Azino-bis (3-ethylbenzthiazoline-6-sulphonic acid) (ABTS) was a product of Tokyo Kasei. Kogyo. (Tokyo, Japan). Ni-NTA HRP Conjugate was from QIAGEN (Hilden, Germany). A 96-well ELISA plate (SUMILON®, MS-8696F) was purchased from Sumitomo Bakelite (Tokyo, Japan).

Binding assay of rsRAGE to rhHMGB1 or rhS100A12. A flat-bottom 96-well plate was coated overnight with various concentrations of rhHMGB1 or rhS100A12 at 4°C (50μl/well). Control wells received only PBS (50μl/well). The plates were washed with PBS (200μl/well) 3 times and blocked with 10% (w/v) BSA in PBS (100μl/well) for 2h at room temperature. After unbound rhHMGB1 or rhS100A12 was washed off, different concentrations of rsRAGE diluted with 10% BSA in PBS were

added into wells in triplicate (50 μl/well), and incubation continued overnight at 4°C. Unbound rsRAGE was removed by washing 3 times with PBS at room temperature. Ni-NTA HRP Conjugate 1/500 diluted by 0.2% BSA in PBS (100 μl/well) was added to the wells and incubated for 2h at 4°C. After washing with PBS, substrate solution, 0.1% ABTS dissolved in 20mM phosphate-citrate buffer (pH 5.0) was added to each well (50 μl/well) and incubated for 30min at room temperature. Finally, a stop solution of 1% SDS was added (100 μl/well). The absorbance was measured at 415nm in a microplate reader (Model 680) from Bio-Rad Laboratories (Hercules, CA, USA).

To determine the effects of divalent cations on the binding, experiments for rsRAGE binding to rhHMGB1 were performed with PBS buffer containing no divalent cations; 1mM $CaCl_2$; 1mM $CaCl_2$ and 10 μM $ZnCl_2$ throughout, and the experiments for rsRAGE binding to rhS100A12 were performed with PBS buffer containing no divalent cations; 1mM $CaCl_2$; 1mM $CaCl_2$ and 0.5mM $MgCl_2$; 1mM $CaCl_2$ and 10 μM $ZnCl_2$; 1mM $CaCl_2$ and 0.5mM $MgCl_2$ and 10 μM $ZnCl_2$ throughout. rsRAGE and rhHMGB1 were incubated for 24h, 48h, and 72h at 4°C, respectively, to determine the effect of incubation time on the binding of rsRAGE to rhHMGB1.

rsRAGE was purified by heparin-sepharose affinity chromatography. rsRAGE, partially purified by using a Ni-NTA column, was further purified by heparin-sepharose affinity chromatography. Heparin-sepharose CL-6B (GE Healthcare, Milwaukee, WI, USA) was poured into the column and equilibrated with 20mM phosphate buffer (pH 7.4) containing 150mM NaCl. rsRAGE was mixed with heparin-sepharose for 3h at 4°C. The supernatant was removed after centrifugation for 15min at 1,500rpm. rsRAGE was eluted with buffer containing 600mM NaCl after washing with buffer containing 150mM NaCl. Purified rsRAGE was analyzed by SDS-PAGE.

Binding of rhS100A12 to heparin-sepharose. 100 μl of 50% heparin-sepharose slurry was washed with 200 μl PBS by centrifugation at 1,500rpm for 5min twice. PBS containing 1mM EDTA, no divalent cations, or 1mM Ca^{2+} was used throughout the experiment. To the washed gel was added 200 μl of rhS100A12. Samples were mixed in rotation at 4°C for 3h. The supernatant and the sepharose gel were incubated with SDS-PAGE sample buffer at 99°C for 5min in a shaker. Then, 15 μl of each sample was electrophoresed by SDS-PAGE.

The effects of different preparations of heparin with diverse molecular weights on the binding of rsRAGE to rhHMGB1 or rhS100A12. rhHMGB1 or rhS100A12 was coated on the plate as described above. Then, 25 μg/ml rsRAGE was incubated with various concentration of heparin preparations diluted by 10% BSA in PBS for 30min at 4°C, and the mixture was added to the plate (50 μl/well). The following procedures were the same as those described above in the binding assay.

Results

rsRAGE binding to rhHMGB1. Different concentrations of rhHMGB1 were immobilized on 96-well plates, and then various concentrations of rsRAGE were added to the plate. Bound sRAGE was determined by the addition of Ni-NTA HRP followed by the peroxidase reaction. The total binding was dependent on both rhHMGB1 and rsRAGE (Fig. 1A). The binding was saturable with respect to the rsRAGE concentration (Fig. 1B). The values of nonspecific binding in the absence of rhHMGB1 were very small compared with the specific binding. The inset shows a Scatchard plot of the specific binding obtained with rhHMGB1 at 6 μg/ml for coating. The K_d value of sRAGE for rhHMGB1 determined from the Scatchard analysis was 0.71 μM. rsRAGE bound to rhHMGB1 also in a time-dependent manner (Fig. 2). The presence of Ca^{2+} (1mM) on the combination did not influence the binding of rsRAGE to rhHMGB1 (Fig. 3).

rsRAGE binding to rhS100A12. Since S100A12 has been demonstrated to be a Ca^{2+}- and Zn^{2+}-binding EF-hand protein [28], we examined the effects of divalent cations on rsRAGE binding to rhS100A12. Ca^{2+} (1mM) alone significantly increased the binding of rsRAGE to rhS100A12, by 3-fold. Zn^{2+} (10 μM) further enhanced binding, while Mg^{2+} (0.5mM) had no effect on it (Fig. 4). These results implied that Ca^{2+}- and Zn^{2+}-bound conformation of S100A12 is required for the optimal binding to rsRAGE. Fig. 5A shows the total and specific binding of rsRAGE to immobilized rhS100A12 (2 μg/ml, 10 μg/ml, and 50 μg/ml for the coating plate) in the

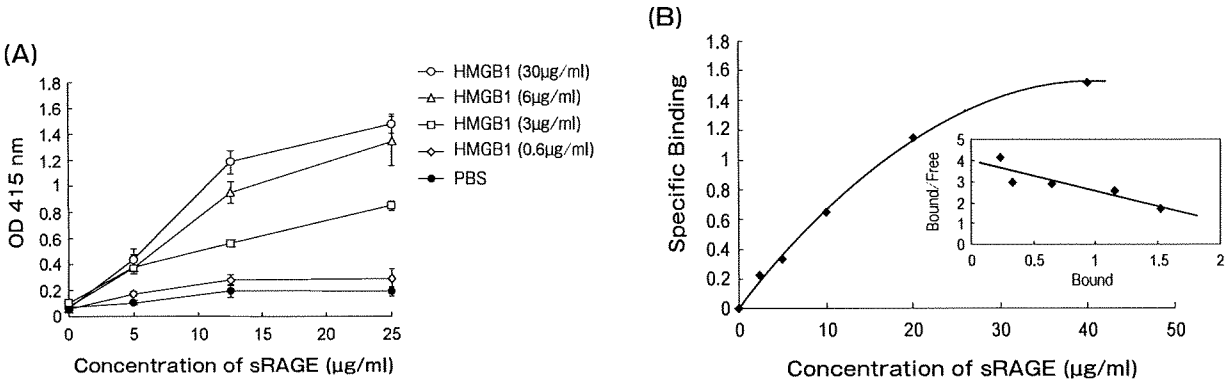

Fig. 1 Concentration-dependent binding of rsRAGE to rhHMGB1. (A) Different concentrations of rhHMGB1 were immobilized onto the wells of a 96-well plate. After blocking the plate with 10% BSA/PBS, the indicated concentrations of rsRAGE were added to the wells. The bound rsRAGE was quantified as described in Methods. The results were the means ± SEM of 3 independent experiments. (B) Specific binding of rsRAGE to rhHMGB1 was calculated by subtracting nonspecific binding in the absence of rhHMGB1 from the total binding with 6μg/ml of rhHMGB1. The inset shows the Scatchard plot of the saturation curve. The K_d value of rsRAGE for rhHMGB1 binding was estimated to be 0.71μM.

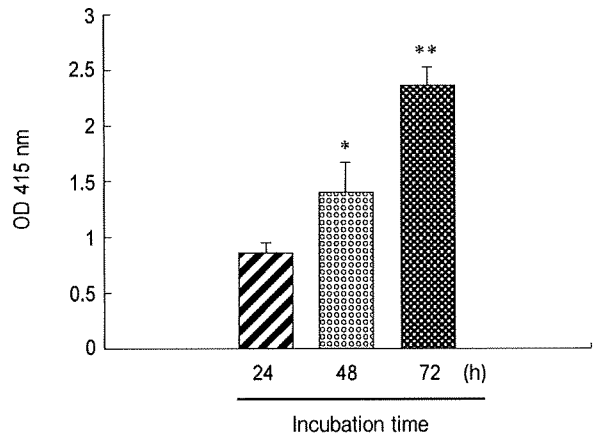

Fig. 2 Time-dependent binding of rsRAGE to rhHMGB1. First, 3μg/ml of rhHMGB1 was immobilized onto each well of a 96-well plate. After the plate was blocked with 10% BSA/PBS, 25μg/ml of rsRAGE was added to each well and the incubation continued for 24h, 48h, and 72h at 4°C. The results were the means ± SEM of 3 independent experiments. $^*P<0.05$, $^{**}P<0.01$ compared with the value at 24h.

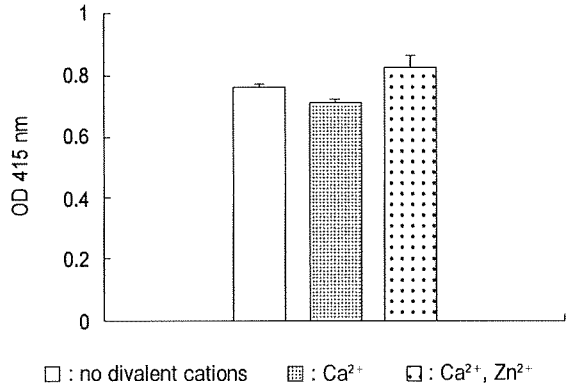

Fig. 3 The effects of Ca^{2+} and Zn^{2+} on rsRAGE binding to rhHMGB1. The plate was coated with 6μg/ml rhHMGB1, and 12.5μg/ml rsRAGE was added to each well. 1mM Ca^{2+} and 10μM Zn^{2+} were added to the well indicated at the start of plate coating and were present throughout the period immediately before the final reaction. The results were the means ± SEM of 3 independent experiments.

presence of Ca^{2+} and Zn^{2+}. The K_d value of rsRAGE for rhS100A12 binding was determined to be 1.39μM by Scatchard analysis, as shown in the inset (Fig. 5B).

rsRAGE was purified by heparin-sepharose affinity chromatography. The fractions obtained from heparin-sepharose affinity chromatography were run on SDS-PAGE gels under denaturing conditions. Coomassie brilliant blue staining showed the presence of rsRAGE with a molecular size of 45000 Da (Fig. 6), which strongly suggested that rsRAGE can be regarded as a heparin-binding protein.

rhS100A12 binding to heparin-sepharose. After rhS100A12 was incubated with heparin-sepharose, the supernatant and the sepharose gel were analyzed by SDS-PAGE under denaturing conditions and

Coomassie brilliant blue staining. rhS100A12 bound to heparin-sepharose also in a Ca^{2+}-dependent manner. A band was obtained with a molecular size of 11000 Da in the presence of Ca^{2+}, while there was no clear band in the presence of EDTA or in the absence of Ca^{2+} (Fig. 7).

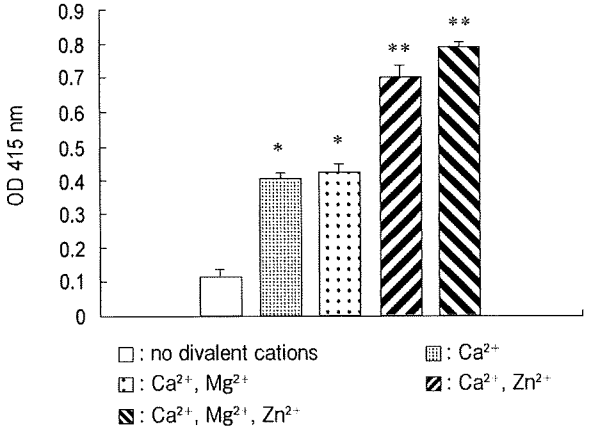

Fig. 4 The effects of divalent cations on rsRAGE binding to rhS100A12. The plate was coated with 50μg/ml rhS100A12, and 25μg/ml rsRAGE was added to each well. Ca^{2+}, Zn^{2+}, and Mg^{2+} were added to the wells indicated at the start of plate coating and were present throughout the period immediately before the final reaction. The results were the means ± SEM of 3 independent experiments. $^{*}P<0.05$, $^{**}P<0.01$ compared with the value with no divalent cations.

Heparin inhibits the binding of rsRAGE to rhHMGB1. The effects of each of the 3 preparations of heparin with different average molecular weights on rsRAGE binding to rhHMGB1 were examined. The concentrations of rhHMGB1 and rsRAGE were fixed at 3μg/ml and 25μg/ml, respectively. All 3 preparations concentration-dependently inhibited the binding of rsRAGE to rhHMGB1 from 0.5 to 2μg/ml (Fig. 8). The rank order of inhibitory potency was UFH, LMWH 5000 Da, and LMWH 3000 Da.

Heparin inhibits the binding of rsRAGE to rhS100A12. The effects of the 3 preparations of heparin with different average molecular weights on the binding of rsRAGE to rhS100A12 were evaluated in the presence of 1mM Ca^{2+} and 10μM Zn^{2+}. The concentrations of S100A12 and rsRAGE were fixed at 50μg/ml and 25μg/ml, respectively. Similar to the effects on the binding of rhHMGB1 to rsRAGE, all 3 preparations concentration-dependently inhibited the binding of rsRAGE to rhS100A12 (Fig. 9). However, the inhibitory potency against S100A12 binding was much lower than that against HMGB1 binding, and that was common to all 3 preparations. Even at 100μg/ml of heparin, the inhibition was about 50%, irrespective of the preparation.

Discussion

RAGE is a transmembrane protein and has been

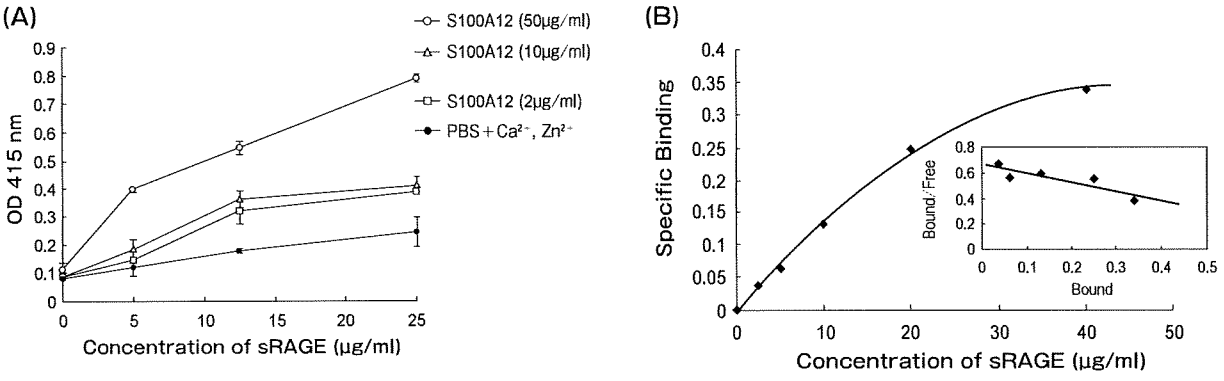

Fig. 5 Concentration-dependent binding of rsRAGE to rhS100A12. (A) Different concentrations of rhS100A12 were immobilized onto the wells of a 96-well plate in the presence of 1mM Ca^{2+}, 10μM Zn^{2+}, and 0.5mM Mg^{2+}. After the plate was blocked with 10% BSA/PBS, the indicated concentrations of rsRAGE were added to the wells. Ca^{2+}, Zn^{2+}, and Mg^{2+} were present throughout the period immediately before the final reaction. The results were the means ± SEM of 3 independent experiments. (B) Specific binding of rsRAGE to rhS100A12 was calculated by subtracting nonspecific binding in the absence of rhHMGB1 from the total binding with 50μg/ml rhS100A12. The inset shows the Scatchard plot of the saturation curve. The K_d value of rsRAGE for rhS100A12 binding was estimated to be 1.39μM.

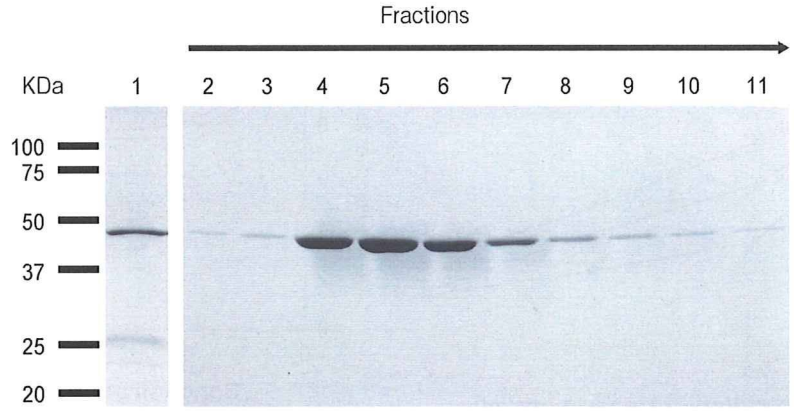

Fig. 6 Purification of rsRAGE using heparin-sepharose affinity chromatography. Partially purified rsRAGE preparations by using a Ni-NTA column (lane 1) were applied to heparin-sepharose. The bound proteins were eluted with 600 mM NaCl (lanes 4-11) after extensive washing (lanes 2 and 3). The eluted samples were electrophoresed on 12% separation gel, and SDS-PAGE gel was stained with Coomassie brilliant blue.

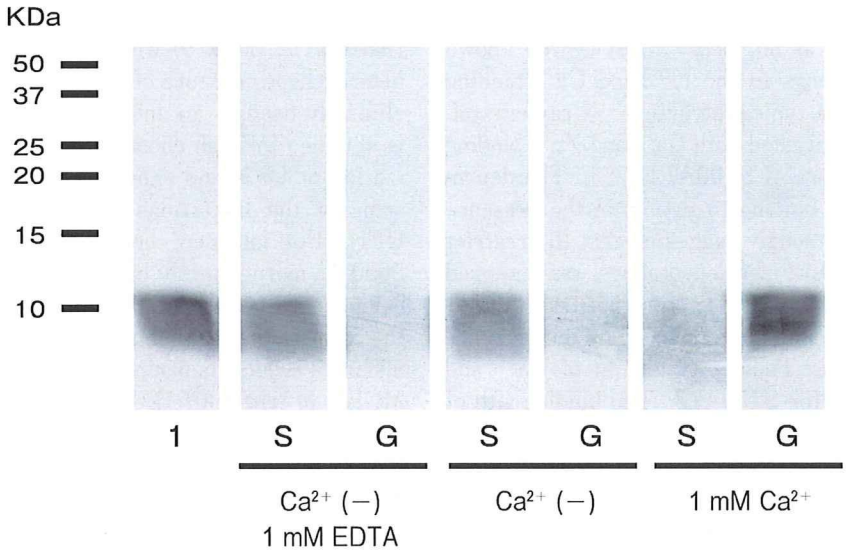

Fig. 7 rhS100A12 binding to heparin-sepharose. rhS100A12 was mixed with heparin-sepharose for 3 h at 4°C under different Ca^{2+} condition. After incubation, the supernatant (S) and the sepharose gel (G) were electrophoresed on 15% separation gel, and the SDS-PAGE gel was stained with Coomassie brilliant blue. Lane 1, loading S100A12.

reported to be a receptor for several ligands including HMGB1, S100A12, S100A8/9, AGEs, and Aβ. RAGE belongs to the immunoglobulin superfamily and has 3 immunoglobulin-like domain structures in the extracellular portion. We used recombinant human soluble RAGE with a 6-histidine tag at the C-terminus for the *in vitro* binding and established the binding assay of HMGB1 or S100A12 to RAGE.

The binding of rhHMGB1 to rsRAGE was concentration-dependent and time-dependent (Fig. 1 and Fig. 2). The binding was saturable in terms of both rhHMGB1 and rsRAGE concentration for constant levels of the pair. rhS100A12 binding to rsRAGE was dependent on divalent cations (Fig. 4 and Fig. 5),

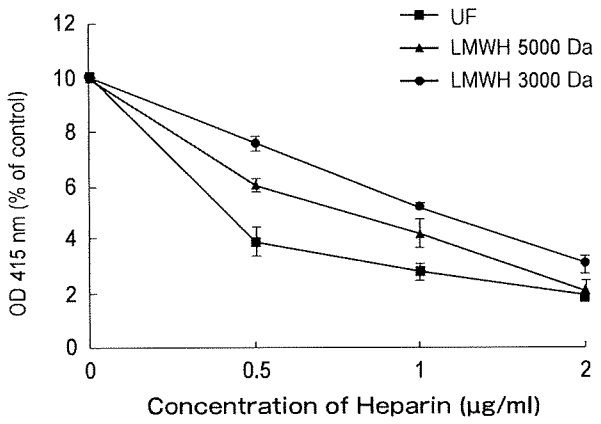

Fig. 8 Effects of heparin with different molecular sizes on rsRAGE binding to rhHMGB1. The different concentrations of UFH (■), LMWH 5000 Da (▲), and LMWH 3000 Da (●) were incubated with 25μg/ml rsRAGE for 30min at 4°C, and the mixture was added to the wells. The results were the mean ± SEM of 3 independent experiments.

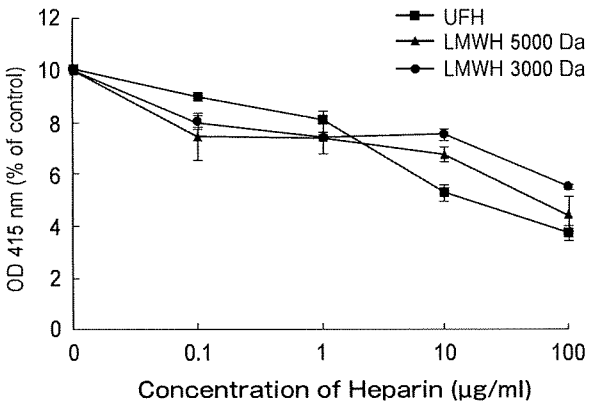

Fig. 9 Effects of heparin with different molecular sizes on rsRAGE binding to rhS100A12. The different concentration of UFH (■), LMWH 5000 Da (▲), and LMWH 3000 Da (●) were incubated with 25μg/ml rsRAGE for 30min at 4°C, and the mixture was added to the wells. The results were the mean ± SEM of 3 independent experiments.

whereas HMGB1 was not (Fig. 3). It is well known that S100A12 belongs to the EF-hand Ca^{2+} binding protein and forms a typical structure. X-ray crystallography analysis revealed both Ca^{2+} and Zn^{2+} binding sites on the structure of S100A12 [25]. The dependence of S100A12 binding to RAGE in the presence of Ca^{2+} and Zn^{2+} strongly suggested that the restrict structure of S100A12 mentioned above was required for its binding to RAGE. In contrast, rhHMGB1 binding to rsRAGE was not influenced by the presence of divalent cations. Thus, the effects of Ca^{2+} and Zn^{2+} were specific for S100A12. The binding site of HMGB1 or S100A12 on RAGE has been postulated from crystallographic studies. Hofmann *et al.* [26] suggested that S100A12 may bind to the V-domain of RAGE. On the other hand, there is controversy as to the binding site of HMGB1 on RAGE. Apparently, the affinity of HMGB1 ($K_d = 0.71\mu M$) to RAGE was higher than that of S100A12 ($K_d = 1.39\mu M$).

Since rsRAGE was able to be purified by heparin-sepharose affinity chromatography (Fig. 6), it was considered to bind to heparin, and rhS100A12 was also found to bind to heparin in the presence of Ca^{2+} (Fig. 7). By using the binding assay, we reported for the first time that heparin had inhibitory effects on the binding of rsRAGE to rhHMGB1 or rhS100A12. Dose-dependent inhibitory effects of UFH and LMWH on the binding of rsRAGE to rhHMGB1 (Fig. 8) or rhS100A12 (Fig. 9) were demonstrated. UFH is a heterogeneous mixture of polysaccharides and has been clinically used as an anticoagulant. LMWH 5000 Da is obtained through chemical or enzymatic depolymerization of UFH and shows advantages in overcoming some of the limitations associated with the use of UFH. For instance, compared with UFH, LMWH 5000 Da more potently inhibits factor Xa, an essential component of the prothrombinase complex leading to the formation of thrombin [27–30]. The exact mechanisms by which heparin blocks the binding of rhHMGB1 or rhS100A12 to rsRAGE remain unclear under this situation. Considering that HMGB1 and RAGE are all heparin-binding proteins [21, 22–24], we hypothesize that one blocking mechanism could be heparin occupancy of the binding site on rsRAGE and/or rhHMGB1. However, further experiments are necessary for the analysis of molecular interaction between rsRAGE and its ligands.

It has been suggested that heparin functions as an anti-inflammation agent by affecting some components in the inflammatory cascade, such as complement activation, platelet activating factor production [31], and expression of P- and L- selectins [32]. In addition, heparin binds antithrombin III to form a complex capable of inhibiting thrombin proteolytic activity. This inhibition prevents clot formation and allows heparin to be utilized clinically as an anticoagulant

[33]. The concept that coagulation can play a role in the inflammatory response has been well illustrated [34]. In acute inflammatory diseases, like sepsis, inflammatory and coagulation systems coexist in delicate homeostasis [35], augment each other, and combine to influence disease progression [36, 37]. Accordingly, heparin's anti-inflammatory effect may be partly assigned to its own anticoagulant property. The present results imply that another anti-inflammatory mechanism of heparin might be the interference effect on the interaction between RAGE and its ligands.

RAGE has been considered a central player in the inflammatory response [38]. It is expressed at low levels in normal tissues and in the vasculature, but becomes upregulated at sites where its ligands accumulate [39]. The RAGE axis is involved in the pathogenesis of a wide range of inflammatory disorders via the integration of ligands. HMGB1 activated Mac-1 as well as Mac-1-mediated adhesive and migratory functions of neutrophils in a RAGE-dependent manner [40]. Interaction of S100A12 with cellular RAGE on vascular endothelial cells, mononuclear phagocytes, and lymphocytes triggers cellular activation, with the expression of VCAM-1, intercellular adhesion molecule-1 (ICAM-1), and tissue factor (TF) as well as production of pro-inflammatory mediators [15]. Therefore, the interaction between RAGE and its ligands should be a target for inflammation-based disease intervention. The *in vitro* RAGE binding established in the present study will provide a convenient assay system for screening candidate drugs to interfere with the binding between RAGE and HMGB1/S100A12.

References

1. Chavakis T, Bierhaus A and Nawroth PP: RAGE (receptor for advanced glycation end products): a central player in the inflammatory response. Microbes Infect (2004) 6: 1219-1225.
2. Bierhaus A, Stern DM and Nawroth PP: RAGE in inflammation: a new therapeutic target? Curr Opin Investig Drugs (2006) 7: 985-991.
3. Schmidt AM, Vianna M, Gerlach M, Brett J, Ryan J, Kao J, Esposito C, Hegarty H, Hurley W and Clauss M: Isolation and characterization of two binding proteins for advanced glycosylation end products from bovine lung which are present on the endothelial cell surface. J Biol Chem (1992) 267: 14987-14997.
4. Dattilo BM, Fritz G, Leclerc E, Kooi CW, Heizmann CW and Chazin WJ: The extracellular region of the receptor for advanced glycation end products is composed of two independent structural units. Biochemistry (2007) 46: 6957-6970.
5. Yamagishi S, Matsui T and Nakamura K: Kinetics, role and therapeutic implications of endogenous soluble form of receptor for advanced glycation end products (sRAGE) in diabetes. Curr Drug Targets (2007) 8: 1138-1143.
6. Yamagishi S, Nakamura K and Matsui T: Advanced glycation end products (AGEs) and their receptor (RAGE) system in diabetic retinopathy. Curr Drug Discov Technol (2006) 3: 83-88.
7. Unoshima M: Therapeutic effect of anti-HMGB1 antibody and anti-RAGE anibody on SIRS/sepsis. Nippon Rinsho (2004) 62: 2323-2329 in Japanese.
8. Mruthinti S, Schade RF, Harrell DU, Gulati NK, Swamy-Mruthinti S, Lee GP and Buccafusco JJ: Autoimmunity in Alzheimer's disease as evidenced by plasma immunoreactivity against RAGE and Abeta42: complication of diabetes. Curr Alzheimer Res (2006) 3: 229-235.
9. Carroll L, Hannawi S, Marwick T and Thomas R: Rheumatoid arthritis: links with cardiovascular disease and the receptor for advanced glycation end products. Wien Med Wochenschr (2006) 156: 42-52.
10. Sisková A and Wilhelm J: Role of nonenzymatic glycation and oxidative stress on the development of complicated diabetic cataracts. Cesk Fysiol (2000) 49: 16-21 in Czech.
11. Scaffidi P, Misteli T and Bianchi ME: Release of chromatin protein HMGB1 by necrotic cells triggers inflammation. Nature (2002) 418: 191-195.
12. Abraham E, Arcaroli J, Carmody A, Wang H and Tracey KJ: HMG-1 as a mediator of acute lung inflammation. J Immunol (2000) 165: 2950-2954.
13. Zimmer DB, Cornwall EH, Landar A and Song W: The S100 protein family: history, function, and expression. Brain Res Bull (1995) 37: 417-429.
14. Vogl T, Pröpper C, Hartmann M, Strey A, Strupat K, van den Bos C, Sorg C and Roth J: S100A12 is expressed exclusively by granulocytes and acts independently from MRP8 and MRP14. J Biol Chem (1999) 274: 25291-25296.
15. Hofmann MA, Drury S, Fu C, Qu W, Taguchi A, Lu Y, Avila C, Kambham N, Bierhaus A, Nawroth P, Neurath MF, Slattery T, Beach D, McClary J, Nagashima M, Morser J, Stern D and Schmidt AM: RAGE mediates a novel proinflammatory axis: a central cell surface receptor for S100/calgranulin polypeptides. Cell (1999) 97: 889-901.
16. Alban S: Pharmacology of heparins and direct anticoagulants. Hamostaseologie (2008) 28: 400-420.
17. Tefferi A, Owen BA, Nichols WL, Witzig TE and Owen WG: Isolation of a heparin-like anticoagulant from the plasma of a patient with metastatic bladder carcinoma. Blood (1989) 74: 252-254.
18. Tyrell DJ, Kilfeather S and Page CP: Therapeutic uses of heparin beyond its traditional role as an anticoagulant. Trends Pharmacol Sci (1995) 16: 198-204.
19. Gaffney A and Gaffney P: Rheumatoid arthritis and heparin. Br J Rheumatol (1996) 35: 808-809.
20. Prajapati DN, Newcomer JR, Emmons J, Abu-Hajir M and Binion DG: Successful treatment of an acute flare of steroid-resistant Crohn's colitis during pregnancy with unfractionated heparin. Inflamm Bowel Dis (2002) 8: 192-195.
21. Myint KM, Yamamoto Y, Doi T, Kato I, Harashima A, Yonekura H, Watanabe T, Shinohara H, Takeuchi M, Tsuneyama K, Hashimoto N, Asano M, Takasawa S, Okamoto H and Yamamoto H: RAGE control of diabetic nephropathy in a mouse model: effects of RAGE gene disruption and administration of low-molecu-